

MTB-610-89A
AUGUST 16, 1990

EVALUATION OF
HIGH PERFORMANCE METAL ALLOYS
IN THE STS LAUNCH ENVIRONMENT USING
ELECTROCHEMICAL IMPEDANCE SPECTROSCOPY

PREPARED BY:

ENGINEERING DEVELOPMENT DIRECTORATE
MECHANICAL ENGINEERING DIRECTORATE
MATERIALS SCIENCE LABORATORY
MATERIALS TESTING BRANCH

**National Aeronautics and
Space Administration**
John F. Kennedy Space Center



MTB-610-89A
AUGUST 16, 1990

EVALUATION OF
HIGH PERFORMANCE METAL ALLOYS
IN THE STS LAUNCH ENVIRONMENT USING
ELECTROCHEMICAL IMPEDANCE SPECTROSCOPY

PREPARED BY:

ENGINEERING DEVELOPMENT DIRECTORATE
MECHANICAL ENGINEERING DIRECTORATE
MATERIALS SCIENCE LABORATORY
MATERIALS TESTING BRANCH

**National Aeronautics and
Space Administration**
John F. Kennedy Space Center



DOCUMENT NO. MTB-610-89A
DXTE: AUGUST 16, 1990

TEST REPORT

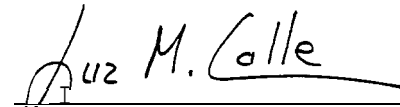
Evaluation of High Performance **Metal** Alloys in the STS Launch Environment Using Electrochemical Impedance Spectroscopy

ISSUED BY

National Aeronautics and Space Administration
Kennedy Space Center
Materials Testing Branch

PREPARED BY:


L. G. MacDowell
Materials Testing Branch



L. M. Calle
NASA/AEE Summer Faculty Fellow

APPROVED BY:


C. L. Springfield, NASA
Chief, Materials Testing Branch

ACKNOWLEDGMENT: The authors wish to thank Ms. K. A. Gorman for the analysis of the electrolyte solution samples using inductively coupled plasma (ICAP) spectrometric methods. This investigation was made possible by the participation of L. M. Calle in the NASA/ASEE Summer Faculty Fellowship Program during the summers of 1989 and 1990.

NOTICE: This document was prepared under the sponsorship of the National Aeronautics and Space Administration. Neither the United States Government nor any person acting on behalf of the United States Government assumes any liability resulting from the use of the information contained in this document, or warrants that such use will be free from privately owned rights.

The citation of manufacturer's names, trademarks or other product identification in this document does not constitute an endorsement or approval of the use of such commercial products.

ABSTRACT

Electrochemical Impedance Spectroscopy (EIS) techniques using AC impedance measurements were chosen to investigate the corrosion resistance of 19 alloys under conditions similar to the Space Transportation System (STS) launch environment. The alloys were: Zirconium 702, Hastelloy C-22, Inconel 625, Hastelloy C-276, Hastelloy C-4, Inconel 600, 7Mo + N, Ferralium 255, Inco Alloy G-3, 20Cb-3, SS 904L, Inconel 825, SS 304LN, SS 316L, SS 317L, ES 2205, SS 304L, Hastelloy B-2, and Monel 400. AC impedance data were gathered for each alloy after one hour immersion time in each of the following three electrolyte solutions: 3.55% NaCl, 3.55% NaCl-0.1N HCl, and 3.55% NaCl-1.0N HCl. The data were analyzed qualitatively using the Nyquist plot and quantitatively using the Bode plot. Polarization resistance, R_p , values were obtained using the Bode plot. Zirconium 702 was the most corrosion resistant alloy in the three electrolytes. The ordering of the other alloys according to their resistance to corrosion varied as the concentration of hydrochloric acid in the electrolyte increased. The corrosion resistance of Zirconium 702 and Ferralium 255 increased as the concentration of hydrochloric acid in the electrolyte increased. The corrosion resistance of the other 17 alloys decreased as the concentration of the hydrochloric acid in the electrolyte increased.

AC impedance data were gathered for 18 of the alloys at various immersion times in 3.55% NaCl-0.1N HCl. Alloy SS 304LN was not included in this part of the investigation because of its similarity to SS 304L and due to time constraints.

Polarization resistance, R_p , values were obtained from the Nyquist plots at each immersion time using the EQUIVALENT CIRCUIT software package available with the 388 Electrochemical Impedance software. Hastelloy C-22 showed the highest overall values for R_p while Monel 400 and Inconel 600 had the lowest overall values. There was good general correlation found between the corrosion performance of the alloys from the beach corrosion testing site and the predicted rate of corrosion that was based on the R_p values obtained in the laboratory. These data suggest that Electrochemical Impedance Spectroscopy can be used to predict the corrosion performance of metal alloys.

TABLE OF CONTENTS

	PAGE
1.0 INTRODUCTION	1
2.0 MATERIALS AND EQUIPMENT	2
2.1 CANDIDATE ALLOYS	2
2.2 AC IMPEDANCE MEASUREMENTS	2
3.0 PROCEDURE FOR AC IMPEDANCE MEASUREMENTS	4
3.1 ONE HOUR IMMERSION IN THREE DIFFERENT ELECTROLYTES	4
3.2 DIFFERENT IMMERSION TIMES IN 3.55% NACL-0.1N HCL	5
4.0 TEST RESULTS AND DISCUSSION	6
4.1 THEORETICAL BACKGROUND	6
4.2 AC IMPEDANCE MEASUREMENTS AFTER ONE HOUR IMMERSION IN THREE DIFFERENT ELECTROLYTES . .	9
4.3 COMPARISON WITH DC POLARIZATION RESULTS	16
4.4 COMPARISON WITH BEACH CORROSION DATA.....	16
4.5 AC IMPEDANCE MEASUREMENTS AT DIFFERENT IMMERSION TIMES IN 3.55% NACL-0.1N HCL.....	17
4.6 COMPARISON WITH BEACH CORROSION DATA.....	21
5.0 CONCLUSIONS	22
5.1 ONE HOUR IMMERSION TIME IN THREE DIFFERENT ELECTROLYTES	22
5.2 VARIOUS IMMERSION TIMES IN 3.55% NACL-0.1N HCL.....	23
6.0 RECOMMENDATIONS	23
REFERENCES	25
APPENDIX A	27
APPENDIX B	37

1.0 INTRODUCTION

- 1.1 Flexible metal hoses are presently used as part of various supply lines that service the Orbiter at the launch pad. These convoluted flexible hoses were originally constructed of 304L stainless steel. The severely corrosive environment at the launch site caused pitting corrosion in many of these flex hoses. In the case of vacuum jacketed cryogenic lines, failure of a flex hose by pitting would cause a localized loss of vacuum and a subsequent localized loss of insulation in that part of the line.
- 1.2 The environment at the launch site is severely corrosive due to the high chloride content caused by the proximity of the Atlantic Ocean, and from the generation of concentrated hydrochloric acid (HCl) as a fuel combustion product from the Solid Rocket Boosters (SRB's) during launch. These corrosive conditions caused severe pitting on some of the commonly used stainless steel alloys.
- 1.3 An investigation was undertaken in 1987 to evaluate 19 metal alloys with the purpose of finding a more corrosion resistant replacement material for 304L stainless steel. Tests performed in that investigation were: electrochemical corrosion testing, accelerated corrosion testing in a salt fog chamber, long term exposure at the beach corrosion testing site, and pitting corrosion tests in ferric chloride solution. These tests led to the conclusion that the most corrosion resistant alloys were, in descending order, Hastelloy C-22, Inconel 625, Hastelloy C-276, Hastelloy C-4, and Inco Alloy G-3. Of these five alloys, the Hastelloy C-22 stood out as being the best of the alloys tested. The details of this investigation are found in report MTB-325-87A (1). Furthermore, when corrosion resistance was combined with weld and mechanical properties, Hastelloy C-22 was determined to be the best material for the fabrication of flex hoses used as part of the fuel lines servicing the Orbiter at the launch site.
- 1.4 The above electrochemical corrosion testing was based on the use of DC polarization techniques. In our present investigation, Electrochemical Impedance Spectroscopy (EIS) techniques using AC impedance measurements were utilized in order to study the corrosion of the same 19 alloys tested in 1987. During the first part of the investigation, the 19 alloys were tested after one hour immersion in three different electrolyte conditions: neutral

3.55% NaCl, 3.55% NaCl-0.1N HCl, and 3.55% NaCl-1.0N HCl. The second part of the investigation involved the study of 18 of the 19 alloys in 3.55% NaCl-0.1N HCl at different immersion times. The 3.55% NaCl-0.1N HCl electrolyte provides an environment similar to the conditions at the launch pad.

2.0 MATERIALS AND EQUIPMENT

2.1 CANDIDATE ALLOYS

The 19 alloys tested and their nominal compositions in weight percent are shown in Table 1. The choice of these alloys for the investigation was based on their advertised resistance to corrosion in chloride environments.

2.2 AC IMPEDANCE MEASUREMENTS

2.2.1 A Model 378 Electrochemical Impedance system manufactured by EG&G Princeton Applied Research Corporation (PARC) was used for all EIS measurements. The system includes: (1) the Model 273 Computer-Controlled Potentiostat/Galvanostat; (2) the Model 5301A Computer-Controlled Lock-In Amplifier; (3) the IBM XT Microcomputer with peripherals; and (4) the Model 378 Electrochemical Impedance Software. An updated version of the software (PARC version 2.7) including circuit modeling routines was used for the EIS measurements at different immersion times.

2.2.2 Specimens were flat coupons 1.59 cm (5/8") in diameter. The PARC flat specimen holder in the electrochemical cell was designed such that the exposed metal surface area is 1 cm².

TABLE 1 CANDIDATE ALLOYS AND THEIR NOMINAL COMPOSITIONS (WT%)

ALLOY	Ni	Fe	Cr	Mo	Mn*	Co*	Cu	C*	Si*	P*	S*	Other
HASTELLOY C-4	Bal.	3.0	18	17	1.0	2.0		0.01	0.08	0.02	0.01	Ti 0.7
HASTELLOY C-22	Bal.	3.0	22	13	0.5	2.5		0.01	0.08	0.02	0.01	V 0.3, W 3
HASTELLOY C-276	Bal.	7.0	17	17	1.0	2.5		0.01	0.08	0.02	0.01	0.3, W 4.5
HASTELLOY B-2	Bal.	2.0	1	28	1.0	1.0		0.01	0.1	0.02	0.01	
INCONEL 600	Bal.	8.0	16		1.0		0.5	0.15	0.5	0.01	0.01	
INCONEL 625	Bal.	5.0	23	10	0.5	1.0		0.10	0.5	0.01	0.01	Cb 4.1
INCONEL 825	Bal.	22.0	21	3	1.0		2.5	0.05	0.5	0.04	0.03	
INCO G-3	Bal.	20.0	22	7	1.0	5.0	2.0	0.02	1.0	0.04	0.03	Cb 0.5, W 1.5
MONEL 400	Bal.	2.5			2.0		31	0.30	0.5		0.02	Zr 99.2, Hf 4.5
ZIRCONIUM 702												
SS 304L	10	Bal.	9		2.0			0.03	1.0			
SS 304LN	10	Bal.	9		2.0			0.03	1.0	0.04	0.03	N 0.13
SS 316L	12	Bal.	7	2.5	2.0			0.03	1.0	0.04	0.03	
SS 317L	13	Bal.	19	3.5	2.0			0.03	1.0			
SS 904L	25	Bal.	21	4.5	2.0		1.5	0.02	1.0	0.04	0.03	
20 Cb-3	35	Bal.	20	2.5	2.0		3.5	0.07	1.0			
7Mo + N	4	Bal.	28	2	2.0			0.03	0.6	0.03	0.01	N 0.25
ES 2205	5	Bal.	22	3	2.0			0.03	1.0	0.03	0.02	N 0.14
FERRALIUM 255	5	Bal.	26	3	1.5		2.0	0.04	1.0	0.04	0.03	N 0.17

* Values are max.

2.2.3 The electrochemical cell included a saturated calomel reference electrode (SCE), 2 graphite rod counter electrodes, a metal working electrode, and a bubbler/vent tube. Each alloy was studied in three different electrolyte conditions after one hour immersion and at different immersion times in aerated 3.55% NaCl-0.1N HCl. The electrolyte conditions for the one hour immersion time were: aerated 3.55% neutral NaCl, aerated 3.55% NaCl-0.1N HCl (similar to the conditions at the launch site), and aerated 3.55% NaCl-1.0N HCl (more aggressive than the conditions at the launch site). All solutions were prepared using deionized water.

3.0 PROCEDURE FOR AC IMPEDANCE MEASUREMENTS

3.1 ONE HOUR IMMERSION IN THREE DIFFERENT ELECTROLYTES

3.1.1 The test specimens were polished with 600-grit paper, wiped with methyl-ethyl ketone, ultrasonically degreased for five minutes in a detergent solution, rinsed with deionized water, and dried. Each specimen was observed under the microscope and weighed before and after each experiment to monitor changes caused by corrosion on its appearance and weight.

3.1.2 The electrolyte solution was aerated with dry air for at least 15 minutes before immersion of the test specimen. Aeration continued throughout the test.

3.1.3 AC impedance measurements were performed under each of the three electrolyte conditions chosen. After immersion in the electrolyte, the sample was allowed to equilibrate for 3600 seconds before the instrument started acquiring data. It was determined previously that after 3600 seconds, the corrosion potential had usually stabilized (2).

3.1.4 The AC impedance measurements were gathered in the frequency range from 100 kHz to 0.1001 Hz to produce Electrochemical Impedance Spectra. A combination of two methods was employed in order to obtain data over the above range of frequencies: (1) phase-sensitive lock-in detection for

measurements from 5 Hz to 100 kHz; and (2) the FFT (Fast Fourier Transform) technique for measurements from 0.1001 Hz to 11 Hz. The data from lock-in (single-sine) and FFT (multi-sine) were automatically merged in the IBM XT microcomputer by the M378 software.

3.1.5 The conditions for the lock-in experiments were: initial frequency, 100 kHz; final frequency, 5 Hz; points/decade, 5; AC amplitude, 5 mV; DC potential, 0 volts (V) vs OC (open circuit); condition time, 0 seconds; condition potential, 0 V vs OC; open circuit delay, 3600 seconds. As a backup, the open circuit potential was also monitored with a high input impedance voltmeter.

3.1.6 The conditions for the FFT experiments were: base frequency, 0.1001 Hz; data cycles, 5; AC amplitude, 10 mV; DC potential, 0 V vs OC; open circuit delay, 0 seconds. The open circuit potential was also monitored with a high input impedance voltmeter.

3.1.7 The data for each experiment were plotted in the Nyquist and Bode plot formats.

3.2 DIFFERENT IMMERSION TIMES IN 3.55% NaCl-0.1N HCl

3.2.1 The test specimens were prepared as described in 3.1.1 and immersed in 3.55% NaCl-0.1N HCl. Aeration continued throughout the test. SS 304LN was excluded from this part of the investigation due to its similarity to SS 304L.

3.2.2 The EIS data were acquired at different immersion times commencing with one hour (zero hours for 304L and Inconel 625). Data were gathered in the frequency range from 100 kHz to 0.001 Hz using the Auto Execute selection of the EG&G PARC M378 Software System version 2.70. Three experiments were performed covering the following frequency ranges: 100 kHz to 5 Hz, 10-0.1 Hz, and 0.1-0.001 Hz. The data from these three experiments were merged automatically. The AC amplitude was 10 mV.

3.2.3 The data for each immersion time were plotted in the Nyquist and Bode plot format.

4.0 TEST RESULTS AND DISCUSSION

4.1 THEORETICAL BACKGROUND

- 4.1.1 AC impedance techniques does offer some distinct advantages over DC techniques (3). First, the small excitation amplitudes, generally in the ranges of 5 to 10 mV peak-to-peak, would cause only minimal perturbations in the electrochemical system, thus reducing errors normally caused by the measuring technique itself. Second, the AC technique offers valuable information about the mechanisms and kinetics of electrochemical processes such as corrosion. Third, measurements can be made in low conductivity solutions where DC techniques are subject to serious potential-control errors.
- 4.1.2 Despite the advantages of the EIS techniques mentioned above, their application requires sophisticated methods in order to interpret the data and thereby extract meaningful results. The application of AC impedance measurements toward the study of corrosion has so far resulted in the publication of large amounts of experimental data without much interpretation. At the present time, the technique is in a transition from the data collection stage to the data analysis stage (4).
- 4.1.3 EIS is based on the presumption that an electrochemical system, such as those studied in this investigation, can be represented by an equivalent electrical circuit. The equivalent circuit for a simple electrochemical cell is shown in Figure 1 (5). The circuit elements R , R_p , and C_{dl} represent, respectively, the uncompensated resistance (resistance from the reference to the working electrode), the polarization resistance (resistance to electrochemical oxidation), and the capacitance close to the metal surface (at the double layer). There are several formats that could be used for the graphical representation of the AC impedance data (3,6,7). Each format offers specific advantages for revealing certain characteristics of a given test system. It was evident from the beginning that the most

suitable formats for plotting the AC impedance data were the Nyquist and the Bode plots.

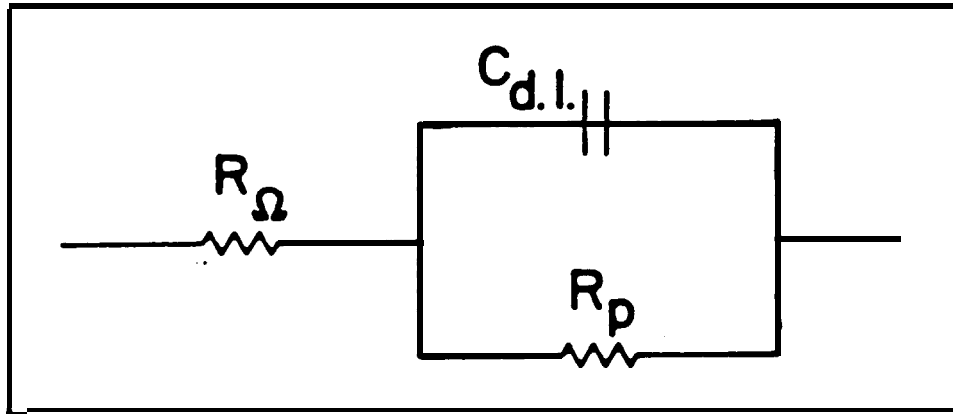


Figure 1. Equivalent circuit for a simple electrochemical cell.

4.1.4 The Nyquist plot is also known as a Cole-Cole plot or a complex impedance plane diagram. Figure 2 (5) shows the Nyquist plot for the equivalent circuit shown in Figure 1. The imaginary component of the impedance (Z'') is plotted versus the real component of the impedance (Z') for each excitation frequency. As indicated in Figure 2, this plot can be used to calculate the values of R , R_p , and C_{d1} .

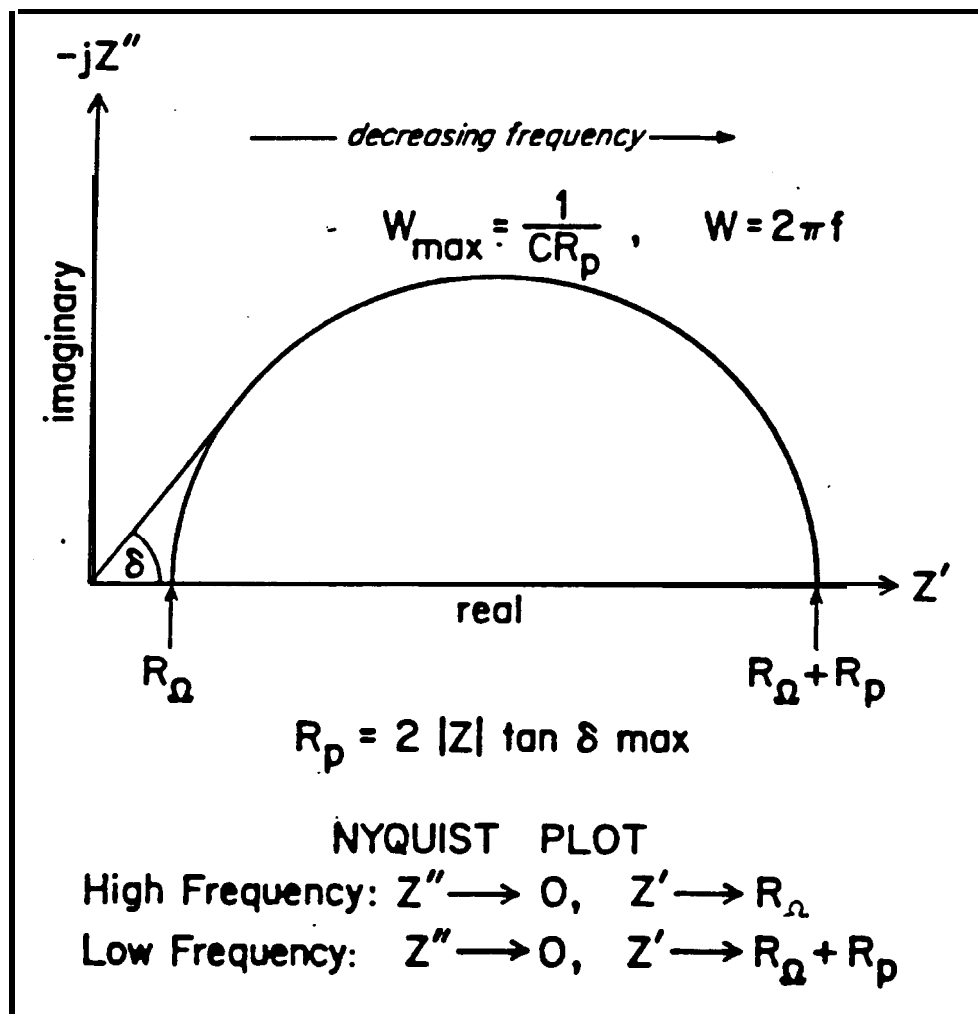


Figure 2. Nyquist plot for equivalent circuit in Figure 1.

4.1.5 The Bode plot for the equivalent circuit in Figure 1 is shown in Figure 3 (5). This graphical representation of the AC impedance data involves plotting both the phase angle (ϕ) and the log of absolute impedance ($\log|Z|$) versus the log of the frequency ($w = 2\pi f$). As indicated on the figure, values for R_{Ω} , R_p , and C_{dl} can also be obtained from the Bode plot. Of special interest for this research is the determination of the R_p values which can be used to calculate the corrosion rate of an electrode material in a given electrolyte (3,8).

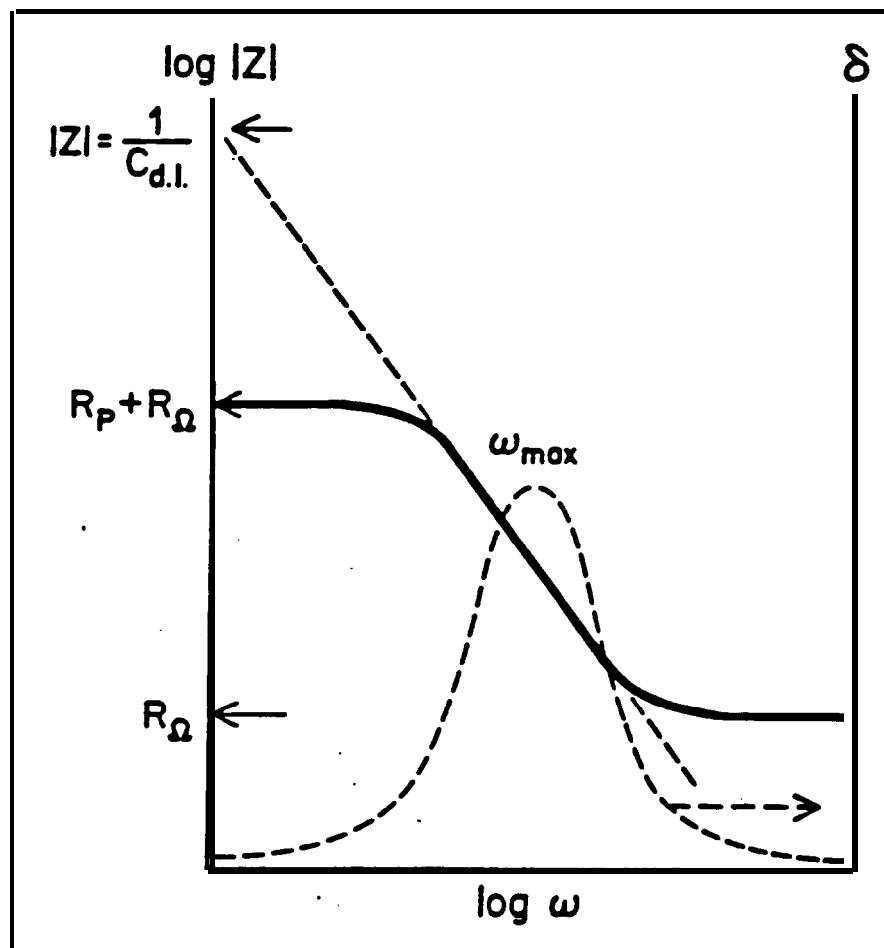


Figure 3. Bode plot for equivalent circuit in Figure 1.

4.2 AC IMPEDANCE MEASUREMENTS AFTER ONE HOUR IMMERSION IN THREE DIFFERENT ELECTROLYTES

4.2.1 The Bode plots included in this report appear in the form of two separate graphs: $\log|Z|$ versus \log Frequency (Hz) and θ versus \log Frequency (Hz). Nyquist (at the top) and Bode plots (at the bottom) for the 19 alloys used in this investigation are shown in Appendix A. None of the Nyquist plots obtained in this investigation exhibited the ideal semicircle shown in Figure 2. Experimentally, it was observed

that deviations from the results predicted using simple equivalent circuits did occur with real, corroding systems (6,9). Some of the deviations that have been observed for real systems are: a semicircle with its center depressed below the real axis, a partial semicircle, and a partial semicircle that changes shape at the low frequency end. EIS data that result in a Nyquist plot in the form of a depressed or partial semicircle could still be used to calculate R_p values. Several authors have described computer modeling of electrochemical impedance (10,11). The usual approach is to curve-fit the semicircle that results from a single time constant capacitive response. This approach allows an estimate to be made of the low frequency intersection of the semicircle response with the real axis. This procedure is especially important when the response still offers a large imaginary contribution at low frequency resulting in a partial semicircle. Deviations that result in a Nyquist plot with the shape of a partial semicircle that changes at the low frequency end would require a more complex computer program with more circuit elements. The time constraint of completing this research project prevented the use of the above methods in analyzing the Nyquist plots for the 19 alloys.

- 4.2.2 Valuable qualitative information could be extracted by comparing the Nyquist plots shown in Appendix A. Each Figure shows the change in the Nyquist plot for a one hour immersion time of the alloy in the three different electrolytes: (X) 3.55% NaCl, (□) 3.55% NaCl-0.1N HCl and (o) 3.55% NaCl-1.0N HCl. The change in the corrosion rate, which is inversely proportional to R_p , could be estimated qualitatively by looking at the change in the Nyquist plot.
- 4.2.3 Zirconium 702 (Figure A-1a) stands out as being the most corrosion resistant alloy under the conditions used in this study. Its R_p was not only the highest but it also showed the least change upon increasing the concentration of the hydrochloric acid from 0.0N to 0.1N to 1.0N. That is, Zirconium 702 became more corrosion resistant as the concentration of hydrochloric acid increased. This finding agrees with the

known fact that Zirconium is resistant to hydrochloric acid at all concentrations up to boiling temperatures. However, there are indications that the metal is vulnerable to pitting in sea water (12).

4.2.4 Ferralium 255 (Figure A-1b) also became more corrosion resistant upon increasing concentrations of the acid. Its R_p values were similar in all three electrolytes but lower than those for Zirconium 702. The change in R_p for the other 17 alloys was in the opposite direction to that observed for Zirconium 702 and Ferralium 255: they became less resistant to corrosion as the concentration of the acid increased. Hastelloy C-22 (Figure A-2a), Inco Alloy G-3 (Figure A-2b), Hastelloy C-4 (Figure A-3a), Inconel 625 (Figure A-3b), Hastelloy C-276 (Figure A-4a), and Hastelloy B-2 (Figure A-4b) have similar Nyquist plots showing a decrease in R_p as the concentration of the acid increases. Monel 400 (Figure A-5a) shows partial semicircles with a slight decrease in R_p when increasing the acid concentration. The semicircle obtained in 3.55% NaCl-0.1N HCl has a feature at the end (a straight line with a positive slope) that has been associated with a Warburg impedance (13). This behavior has been compensated by an extra impedance term in the equivalent circuit that is associated with diffusion controlled processes. 20Cb-3, ES 2205, and 7Mo + N (Figures A-5b, A-6a, A-6b) showed patterns in the Nyquist plot where there was no drastic change in the R_p values when the concentration of hydrochloric acid was increased from 0.0N to 0.1N (as indicated by the two parallel lines). However, a significant change in the Nyquist plot became evident when the concentration of the acid was increased to 1.0N that resulted in a considerable decrease in R_p . The turn at the low frequency end of the curve is probably an indication of a diffusion process taking place. SS 304L (Figure A-7a) exhibited a Nyquist plot that is different from all the others. It should be pointed out that one of the experiments involving SS 304L resulted in a partial breakdown of the surface of the metal sample. Data from that experiment was subsequently discarded. The complex Nyquist plot obtained for SS 304L in 3.55%NaCl-1.0N HCl is similar to the

Nyquist plot obtained for a pin-holed coal tar epoxy coating on mild steel (13). SS 304LN (Figure A-7b) showed good resistance to corrosion in neutral 3.55% NaCl but low resistance to corrosion (low R_p values) in 3.55% NaCl-0.1N HCl and 3.55% NaCl-1.0N HCl. Inconel 600 (Figure A-8a) showed a similar behavior. Inconel 825, SS 317L, SS 904L, and SS 316L (Figures A-8b, A-9a, A-9b, A-10a) show a similar behavior indicating good resistance to corrosion in 3.55% NaCl and 3.55% NaCl-0.1N HCl and a considerably lower resistance to corrosion in 3.55% NaCl-1.0N HCl.

- 4.2.5 Since the Nyquist plots obtained in this investigation did not resemble the ideal Nyquist plot shown in Figure 2, calculation of R_p values from those plots was not pursued. The Bode plot presented a more straightforward means of calculating R_p . In a Bode plot, the impedance of a "perfect capacitance" can be represented as a straight line with a slope of -1 and a phase angle of -90° . A "resistor" will plot as a horizontal line for the $\log|Z|$ with a phase angle of 0° . A Warburg impedance is a straight line with a slope of $-1/2$ and a phase angle of -45° (14). The data gathered for the 19 alloys, when plotted in the Bode format (lower plot in Figures A-1 to A-10), was interpreted as shown in Figure 3. The value of Z at the lowest frequency (0.1001 Hz) is the sum of R_p and R while the value of Z at the highest frequency (100.020 kHz) is R . The values for R_p obtained from the Bode plot data after one hour immersion in the three different electrolytes are given in Tables 2-4. These values indicate that Zirconium 702 is the most corrosion resistant alloy under the conditions used in this study. The ranking of the other 18 alloys differs for the three electrolytes. In general, it can be concluded that for all the alloys, with the exception of Zirconium 702 and Ferralium 255, the R_p values decrease as the concentration of hydrochloric acid increases in the electrolyte. The changes in R_p can thus be followed qualitatively by examining the data in the Nyquist plot format and quantitatively by using the Bode plot format.

TABLE 2

POLARIZATION RESISTANCE IN 3.55% NaCl

MATERIAL NAME	Rp (ohms)
ZIRCONIUM 702	60884
HASTELLOY C-22	23146
INCONEL 625	18338
HASTELLOY C-276	17121
HASTELLOY C-4	15797
INCONEL 600	15426
7M0 + N	15394
FERRALIUM 255	15057
INCO ALLOY G-3	14787
20CB-3	14660
ss 904L	14449
INCONEL 825	14237
SS 304N	13103
SS 316L	12598
SS 317L	12290
ES-2205	11913
SS 304L	11383
HASTELLOY B-2	3779
MONEL 400	652

TABLE 3

POLARIZATION RESISTANCE IN 3.55% NaCl-0.1N HCl

MATERIAL NAME	R _p (ohms)
ZIRCONIUM 702	59937
FERRALIUM 255	15675
20CB-3	1 5 3 6 9
SS 317L	14745
SS 316L	14290
INCONEL 625	13798
INCONEL 825	13281
ES-2205	13227
SS 904L	12786
INCO ALLOY G-3	12716
7M0 + N	12502
HASTELLOY C-4	11723
HASTELLOY C-276	10947
HASTELLOY C-22	9758
HASTELLOY B-2	1806
ss 304L	778
MONEL 400	586
SS 304LN	531
INCONEL 600	498

TABLE 4

POLARIZATION RESISTANCE IN 3.55% NaCl-1.0N HCl

MATERIAL NAME	R _p (ohms)
ZIRCONIUM 702	57081
FERRALIUM 255	15133
.INCONEL 625	12213 .
INCO ALLOY G-3	11665
HASTELLOY C-4	8698
HASTELLOY C-276	5201
HASTELLOY C-22	6800
HASTELLOY B-2	1487
MONEL 400	538
INCONEL 825	490
INCONEL 600	481
SS 304LN	431
20CB-3	422
SS 304L	325
SS 904L	300
SS 317L	203
SS 316 L	158
ES-2205	101
7MO + N	49

4.2.6 The one hour immersion data revealed the need to vary the immersion time for each metal alloy and to expand the frequency range of the measurements to 0.001 Hz. The implementation of these changes resulted in a considerable increase in time required to obtain measurements. The time to collect the data changed from one hour and ten minutes to three and a half hours. Section 4.6 below deals with AC impedance measurements in 3.55% NaCl-0.1N HCl at different immersion times.

4.3 COMPARISON WITH DC POLARIZATION RESULTS

A comparison of R_p values obtained in this investigation with R_p values obtained by DC polarization techniques for the same alloys in 3.55% NaCl-0.1N HCl (ref. 2, Table 3) and for 10 of the alloys in 3.55% NaCl-1.0N HCl (ref. 2, Table 9) have shown that there was no similarity found between their respective values of R_p . However, there was good correlation between the two methods when the alloys are rated according to their resistance to corrosion even though ranking does not match exactly. The fact that AC impedance techniques use signals that do not disturb the electrode properties to be measured have added validity to the R_p values obtained by this technique.

4.4 COMPARISON WITH BEACH CORROSION DATA

A comparison of R_p values obtained from AC impedance measurements with beach corrosion data for all the alloys in 3.55% NaCl-1.0N HCl (ref. 2, Figure 9) showed that there was, in general, a good correlation even though the ranking of the metals did not match exactly. For example, Hastelloy C-22 was the most resistant alloy when tested at the beach corrosion site while it ranked only seventh according to the R_p value in this study. It should be pointed out that, as a group, there was good correlation found between the alloys that performed at the top (Zirconium 702, Ferralium 255, Inconel 625, Inco Alloy G-3, Hastelloy C-4, Hastelloy C-276, and Hastelloy C-22) in both investigations. A tentative conclusion that could be drawn from this comparison is that the AC impedance technique could be used to choose candidate materials for possible long-term corrosion testing at the beach testing site. The lack of a close correlation between the AC impedance data and the beach corrosion data may be from the fact that the AC

impedance measurements were obtained after one hour immersion in the aerated electrolytes at room temperature. The conditions at the beach testing site are obviously different (ref. 1, p. 8) and more similar to conditions in the STS launch environment. The results from the present investigation may be more appropriate for testing the corrosion resistance of alloys that are likely to be in contact with liquid electrolytes such as the ones used here.

4.5 AC IMPEDANCE MEASUREMENTS AT DIFFERENT IMMERSION TIMES IN 3.55% NaCl-0.1N HCl

- 4.5.1 The data for this part of the investigation were plotted in the Nyquist and Bode plot format. A close examination of both types of plots revealed that the Nyquist plot provided more information for the 18 alloys at each immersion time and are, therefore, shown in Appendix B. The Bode plots were all very similar in shape and were not included in this report for the sake of brevity.
- 4.5.2 R_p values for the 18 alloys at different immersion times in 3.55% NaCl-0.1N HCl were calculated using the Find Circle option of the Data Cruncher pre-analysis part of the EQUIVALENT CIRCUIT software package available with the Model 388 Electrochemical Impedance Software package. Due to the time constraints imposed on this part of the investigation, a more thorough analysis of the data was not undertaken at this time. The R_p values shown on Table 5 are preliminary and it is anticipated that they will be refined within the near future.

TABLE 5

IMMERSION TIME, POLAR. RESISTANCE (Rp), AND CORR. POTENTIAL (Ecorr)

ALLOY NAME	TIME (hrs)	Rp (ohms)	Ecorr (volts)
HASTELLOY C-4	1	1.9E+05	-0.075
	75	8.2E+05	0.020
	168	1.8E+06	0.478
HASTELLOY C-22	1	2.4E+05	-0.037
	4	4.9E+05	-0.005
	28	3.3E+05	0.080
	122	1.4E+06	0.149
	145	4.9E+05	0.272
	170	3.9E+06	0.224
	192	6.3E+06	0.212
	262	3.5E+07	0.177
	286	6.3E+07	0.159
	312	2.0E+07	0.090
	336	1.4E+08	0.135
	360	2.1E+06	0.135
476	2.1E+06	0.081	
696	8.9E+05	0.115	
HASTELLOY C-276	1	2.0E+05	0.06
	24	8.0E+05	0.05
	144	2.3E+06	0.05
	168	1.0E+06	0.031
HASTELLOY B-2		1.7E+03	-0.134
	32	1.3E+03	-0.133
	120	1.6E+03	-0.118
	192	1.6E+03	-0.124
INCONEL 600	1	4.5E+02	-0.223
	28	8.8E+02	-0.134
	72	6.3E+02	-0.221
	224	7.6E+02	-0.205
	268	6.0E+02	-0.205
INCONEL 625	0	1.8E+05	-0.3-0
	5	5.0E+05	0.138
	31	4.3E+05	0.353
	100	2.5E+05	0.450
	291	1.7E+05	0.451
	395	1.4E+05	0.450

TABLE 5 (cont.)

ALLOY NAME	TIME (hrs)	Rp (ohms)	Ecorr (volts)
INCONEL 825	1	6.2E+05	-0.081
	28	4.9E+05	-0.090
	72	3.2E+06	-0.050
	168	6.5E+05	-0.052
INCO G-3	1	4.5E+05	-0.080
	40	9.4E+05	0.218
	61	1.0E+06	0.242
	88	2.8E+06	0.249
	161	3.3E+06	0.258
	188	3.7E+06	0.254
	331	6.4E+06	0.238
	505	9.6E+06	0.233
MONEL 400	1	9.7E+02	-0.146
	48	6.5E+02	-0.128
	120	5.7E+02	-0.129
	192	6.8E+02	-0.115
ZIRCONIUM 702 SAMPLE 1	1	1.7E+05	-0.088
	24	4.3E+02	-0.049
	48	1.0E+03	0.090
	72	1.1E+01	0.157
SAMPLE 2	3	5.9E+05	-0.1109
	20	7.4E+05	0.136
	43	7.7E+01	0.156
	67	9.9E+00	-0.017
	91	7.6E+01	0.163
	163	3.3E+01	0.152
SS 304L	0	3.8E+02	-0.151
	7	6.5E+02	-0.345
	24	7.8E+02	-0.323
	31	6.2E+02	-0.322
	54	5.0E+05	-0.127
	100	1.3E+05	-0.161
	192	1.4E+05	-0.163
	243	2.3E+05	-0.151

TABLE 5 (cont.)

ALLOT NAME	TIME (hrs)	Rp (ohms)	Ecorr (volts)
SS 316L	1	2.6E+05	-0.117
	48	9.5E+05	-0.077
	120	6.4E+05	-0.140
	192	5.1E+05	-0.120
SS 317L	24	1.4E+06	-0.030
	128	2.1E+06	-0.102
	168	6.5E+06	-0.007
SS 904L	1	6.3E+05	-0.033
	44	4.2E+06	0.022
	120	9.1E+06	0.152
	168	1.6E+06	0.239
20 CB-3	1	3.4E+05	-0.081
	2s	2.9E+06	0.080
	96	8.8E+05	-0.020
	168	1.4E+06	0.019
7 MO + N	1	5.3E+05	-0.122
	25	3.1E+06	-0.020
	90	2.3E+06	-0.113
	115	4.6E+05	-0.176
	137	1.5E+06	-0.111
	161	1.5E+06	-0.130
ES-2205	1	3.0E+05	-0.101
	26	2.0E+06	0.015
	73	9.8E+05	-0.037
	166	7.2E+05	-0.120
FERRALIUM 255	1	4.3E+05	-0.115
	24	7.1E+05	-0.068
	48	2.1E+06	0.003
	120	3.0E+05	-0.209
	124	2.9E+05	-0.239
	151	1.1E+07	-0.002
	175	2.3E+07	0.048
	200	3.7E+07	0.067
	223	8.3E+06	0.071
	393	2.0E+06	0.100
	317	7.4E+02	0.111
	343	5.1E+02	0.126
	367	8.6E+05	0.140
	551	1.3E+07	0.249
634	1.8E+07	0.247	

- 4.5.3 Examination of R_p values for different immersion times revealed that R_p changes differently with time for each alloy. This means that alloys differ significantly in terms of how their rates of corrosion change with immersion time.
- 4.5.4 Hastelloy C-22 showed the highest overall values of R_p while Monel 400 and Inconel 600 had the lowest overall values. Zirconium 702 showed a variation in R_p from 10^5 to 10^1 . Data collection for this sample was very difficult because the instrument would cease to gather data when dark spots, indicative of pitting, appeared on the exposed surface of the sample. This is the reason for having used two samples of this material. It should be noted that Zirconium 702 was found to be the most corrosion resistant alloy in the one-hour immersion time/different electrolyte investigation. The drastic change in the rate of corrosion for this material at different immersion times indicated the importance of performing AC impedance measurements at different immersion times. Other alloys that showed significant changes in the magnitude of R_p with varying immersion times are Ferralium 255 and SS 304L. SS 304L has R_p values indicative of a rate of corrosion that is high at first (low R_p) and then slows down (higher R_p). All the other alloys exhibited R_p values that were on the order of 10^5 to 10^6 .

4.6 COMPARISON WITH BEACH CORROSION DATA

- 4.6.1 A comparison of R_p values obtained in this part of the investigation with beach corrosion data for all the alloys given in Figure 9 of reference 2 indicated that AC impedance measurements could discriminate between the best (Hastelloy C-22) and the worst (Monel 400) performing materials at the beach. There was also good correlation found among the best performing materials as a group (those with the highest R_p values in our study) and the poorest performers (those with the lowest R_p values).
- 4.6.2 There was a discrepancy found between the AC impedance results for 20Cb-3 and its actual performance at the beach corrosion test

site. While its R_p values would predict a low rate of corrosion, this material exhibited one of the two highest rates of corrosion at the beach. A possible explanation for this discrepancy could be obtained by examining the one-hour immersion time data in three different electrolytes (Figure A-5b). The Nyquist plots on this Figure clearly showed the effect on the R_p value caused by increasing the concentration of HCl. While R_p is high for one hour immersion in neutral 3.55% NaCl and in 3.55% NaCl-0.1N HCl, a considerable decrease is observed when the concentration of HCl is increased to 1.0N. It should be noted that the samples at the beach test site were periodically sprayed with 10% HCl which is a higher concentration than the 0.1N used in this part of the investigation.

5.0 CONCLUSIONS

5.1 ONE HOUR IMMERSION TIME IN THREE DIFFERENT ELECTROLYTES

- 5.1.1 AC impedance techniques, when used for corrosion testing, provided useful qualitative (Nyquist plot) and quantitative (R_p values) information that could be used to screen alloys to be subjected to long-term corrosion testing.
- 5.1.2 The R_p values obtained for the 19 alloys under three different electrolyte conditions could be used to rank the alloys according to their resistance to corrosion since R_p is inversely proportional to the rate of corrosion.
- 5.1.3 Zirconium 702 was found to be the most corrosion resistant alloy under the conditions used in this investigation.
- 5.1.4 There was a good general agreement between the results obtained using DC and AC techniques even though the actual R_p values were found to be different. It is believed that the R_p values obtained by the AC technique are more accurate.

5.2 VARIOUS IMMERSION TIMES IN 3.55% NaCl-0.1N HCL

- 5.2.1 AC impedance measurements in 3.55% NaCl-0.1N HCl at different immersion times revealed that the rate of corrosion, as indicated by the R_p values obtained, varies with time for the 18 alloys included in this part of the investigation.
- 5.2.2 An examination of the overall R_p values for each alloy over a range of different immersion times enabled the prediction of the long-term performance of the alloys under similar conditions.
- 5.2.3 AC impedance measurements could be used to rank high performance metal alloys according to their rate of corrosion in order to distinguish between those materials expected to have a low rate of corrosion (high R_p) and those expected to have a high rate of corrosion (low R_p).
- 5.2.4 AC impedance measurements, like those reported in this investigation, did not provide the information necessary to discriminate the corrosion rates of the different metal alloys in a way that allows for ranking them exactly according to their rate of corrosion.
- 5.2.5 This part of the investigation revealed the importance of performing AC impedance measurements at different immersion times in order to predict the long-term performance of the metal alloys under similar conditions.

6.0 RECOMMENDATIONS

- 6.1 A further analysis of the data using the full capabilities of the EQUIVALENT CIRCUIT software package.
- 6.2 Include testing of alloys after exposure to conditions that are as similar to the STS launch environment as possible.
- 6.3 Study the effect of protective coatings on the rate of corrosion on the 19 alloys.
- 6.4 Modify the electrolyte conditions to include other chemicals normally found at the STS launch environment.

- 6.5 Study the effect of changes in temperature, similar to the seasonal changes that occur at the STS launch environment, on the rate of corrosion.

REFERENCES

1. MacDowell, L.G. and Ontiveros, C., Evaluation of Candidate Alloys for the Construction of Metal Flex Hoses in the STS Launch Environment, Test Report, Document No. MTB-325-87A, National Aeronautics and Space Administration, Kennedy Space Center, Materials Testing Branch, August 23, 1988.
2. Ontiveros, C., Localized Corrosion of Candidate Alloys for Construction of Fles Hoses, 1987 NASA/ASEE Summer Faculty Fellowship Program Research Reports, Kennedy Space Center, 1987.
3. Application Note XC-1, Basics of AC Impedance Measurements, EG&G PARC, Princeton, NJ., 1981.
4. Yansfeld, F., Don't Be Afraid of Electrochemical Techniques -But Use Them with Care!, Corrosion, Vol. 44, pp. 856-868, 1988.
3. Rothstein, M.L., Electrochemical Corrosion Measurements for the Metal Finishing Industry, Application Note Corr-5, EG&G PXRC, Princeton, NJ., 1986.
6. Mansfeld, F., Recording and Analysis of XC Impedance Data for Corrosion Studies. I. Background and Methods of Analysis, Corrosion, Vol. 37, pp. 301-307, 1981.
7. Mansfeld, F., Kendig, M.W., and Tsai, S., Recording and Analysis of AC Impedance Data for Corrosion Studies. II. Esperimental Approach and Results, Vol. 28, pp. 570-580, 1982.
8. Lorenz, W.J. and Yansfeld, F., Determination of Corrosion Rates by Electrochemical DC and AC Methods, Corrosion Science, Vol. 21, pp. 647-672, 1981.
3. Williams, D.E. and Naish, C.C., An Introduction to the AC Impedance Technique, and its Application to Corroaion Problems, U.K. Atomic Energy Authority, Harwell Report AERE-M3461, pp. 1-10, 1985.
10. Moody, J.R., Quin, S.P., and Strutt, J.E., The Application of a Computerized impedance Monitoring System to a Study of the Behavior of 347 ss in Nitric Acid, presented at the 166th Meeting of the Electrochemical Society, New Orleans, Louisiana, 1984.
11. Kendig, M.W., Meyer, E.M., Lindberg, G. and Yansfeld, F., A Computer Analysis of Electrochemical Impedance Data, Corrosion Science, Vol. 23, pp. 1007-1015, 1982.
12. Uhlig, H.H., Corrosion and Corrosion Control.. An

Introduction to corrosion science and engineering,
Second Edition, John Wiley & Sons Inc., p. 368, 1971.

13. Scantlebury, J.D., Ho, K.N. and Eden, D.A., Impedance Measurements on Organic Coatings on Mild Steel in Sodium Chloride Solutions, Electrochemical Corrosion Testing, ASTM STP 727, Mansfeld, F. and Bertocci, U., Eds., American Society for Testing and Materials, pp. 187-197, 1981.
14. Cahan, B.D. and Chien, C., The Nature of the Passive Film of Iron. II. A-C Impedance Studies, J. Electrochem. Soc., Vol. 129, pp. 474-480, 1982.

APPENDIX A

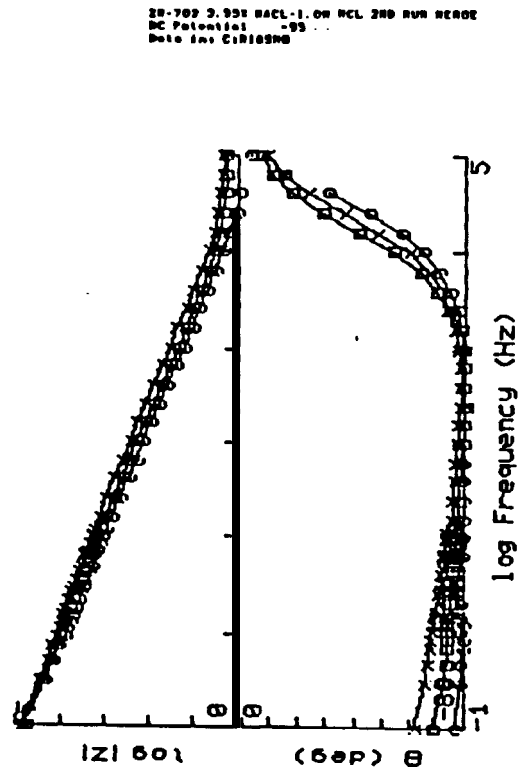
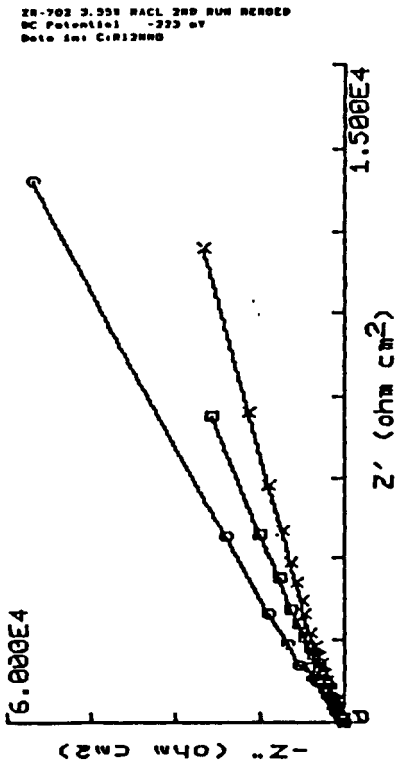
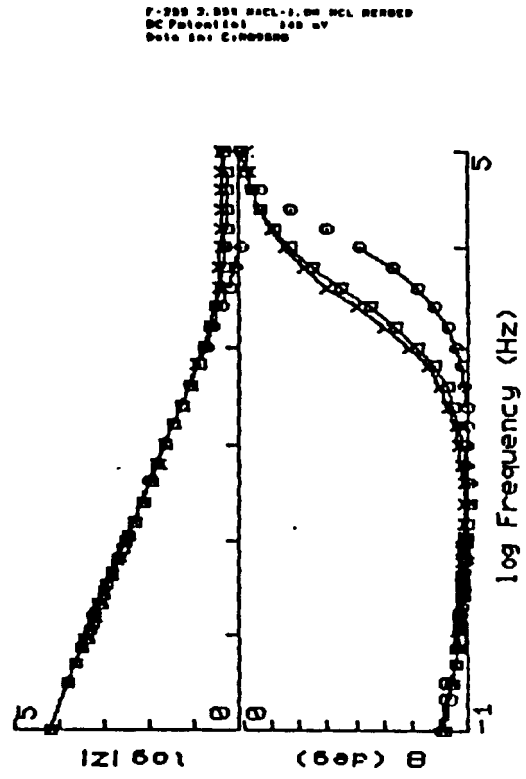
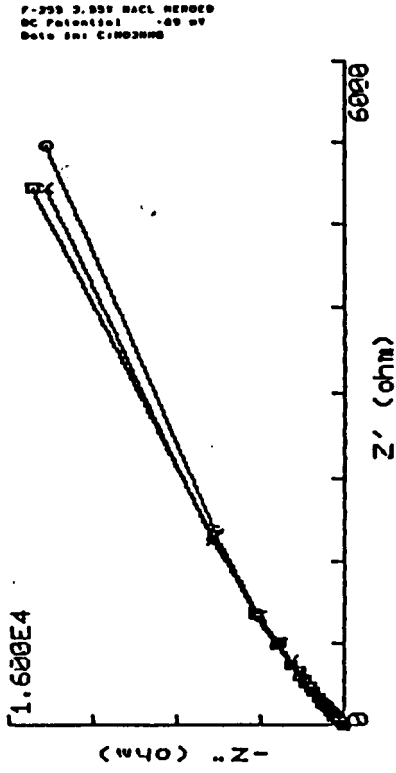
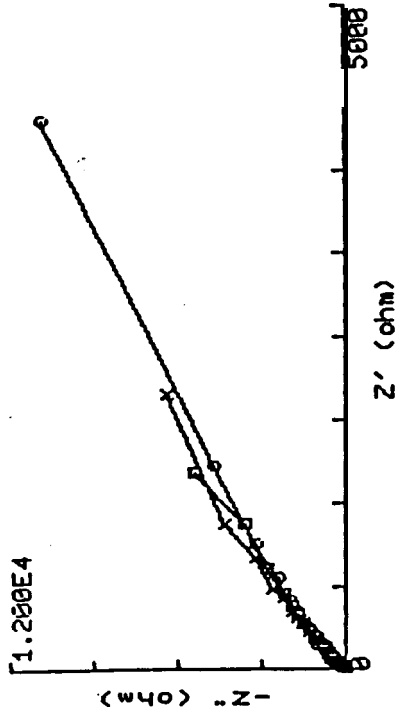
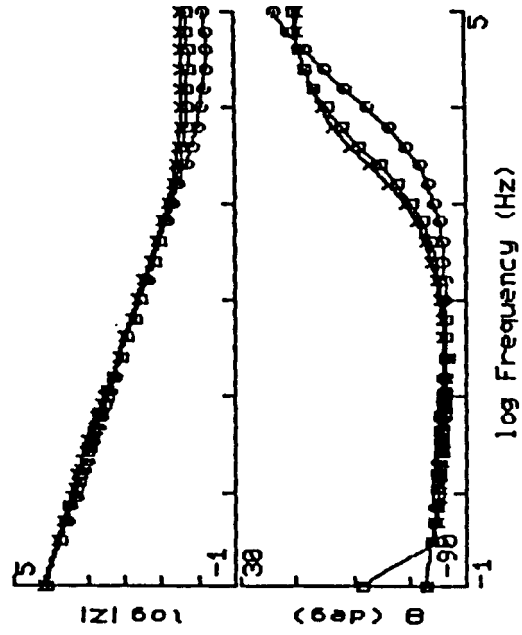


Figure A-1 Nyquist and Bode Plots for Zirconium 702 (a,c) and Ferralium 255 (b,d)

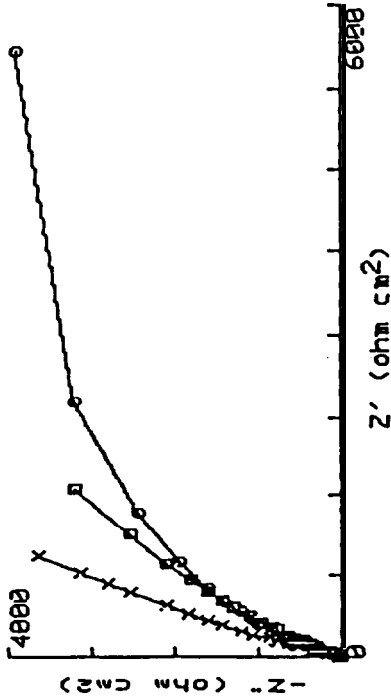
G-3 3.95% NaCl HERDED
DC Potential: -130 mV
Data In: C:003H00



G-3 3.95% NaCl HERDED
DC Potential: -130 mV
Data In: C:003H00



C-22 3.95% NaCl REV PROC HERDED
DC Potential: -42 mV
Data In: C:003H00



C-22 3.95% NaCl-1.0M NaCl HERDED
DC Potential: -110 mV
Data In: C:003H00

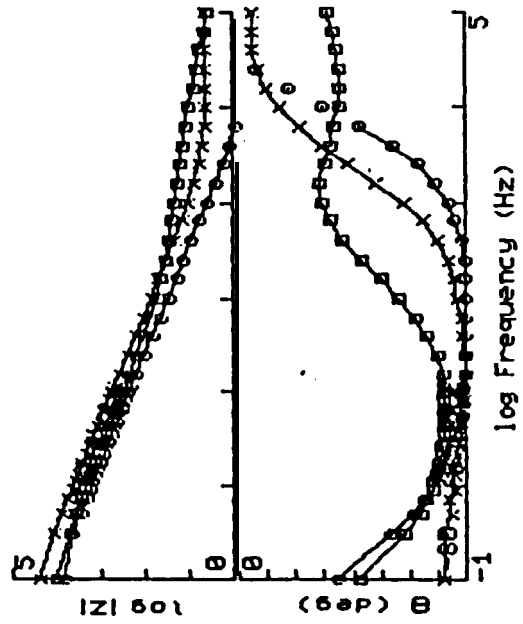


Figure A-2 Nyquist and Bode Plots for Hastelloy C-22 (a,c) and Inco Alloy G-3 (b,d)

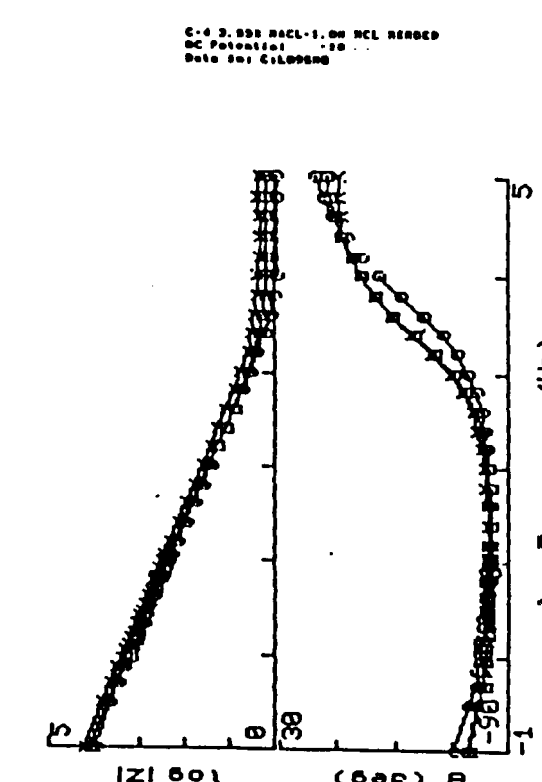
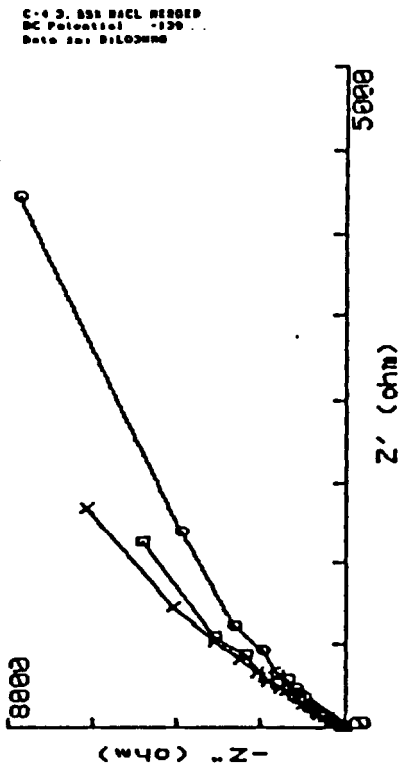
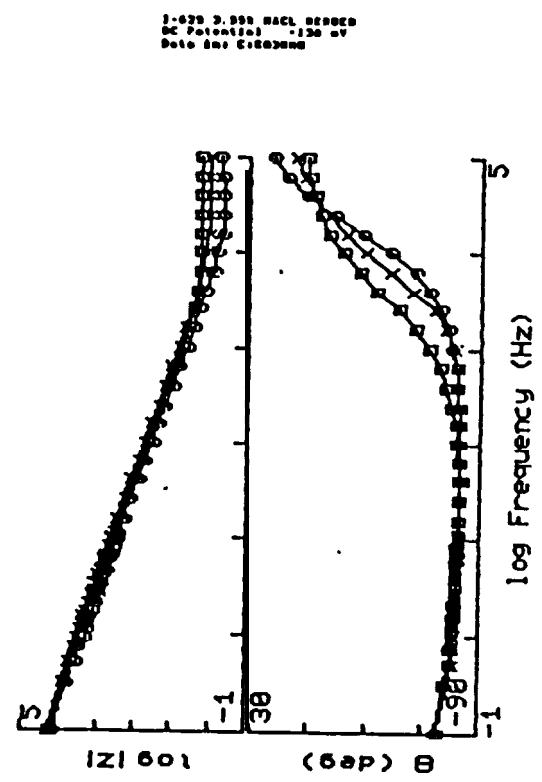
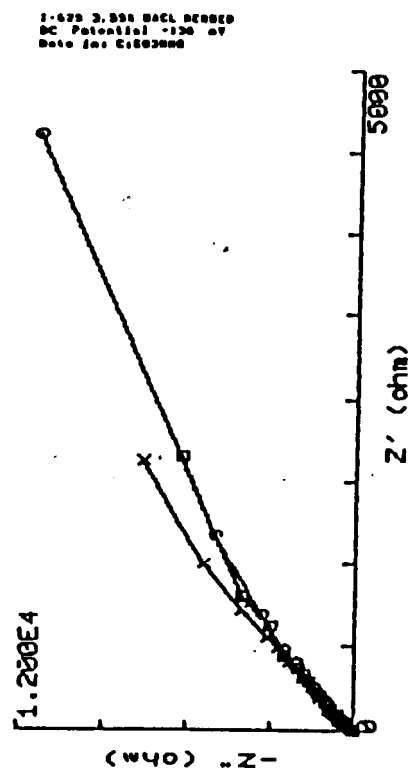


Figure A-3 Nyquist and Bode Plots for Hastelloy C-4 (a,c) and Inconel 625 (b,d)

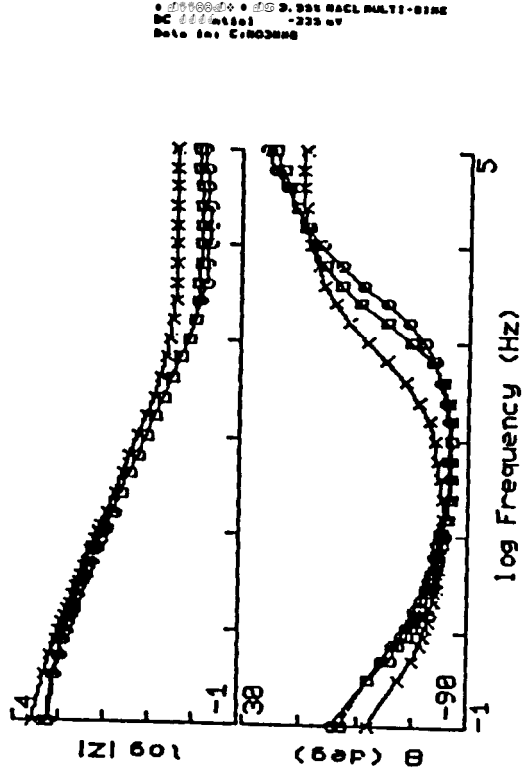
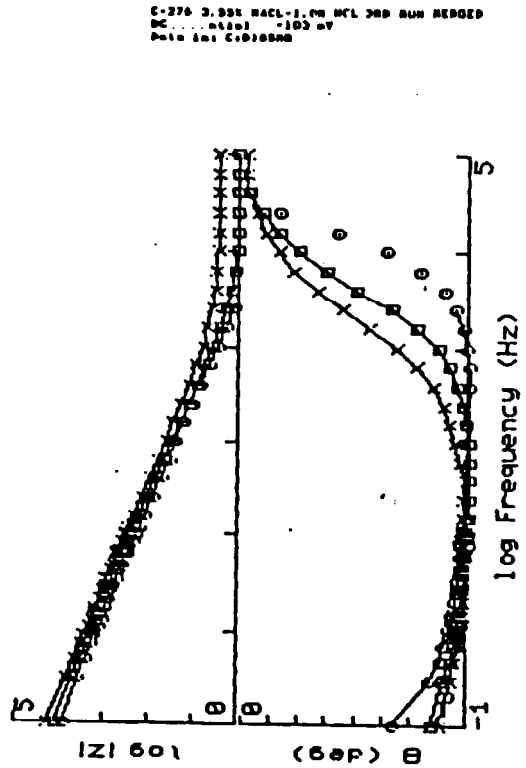
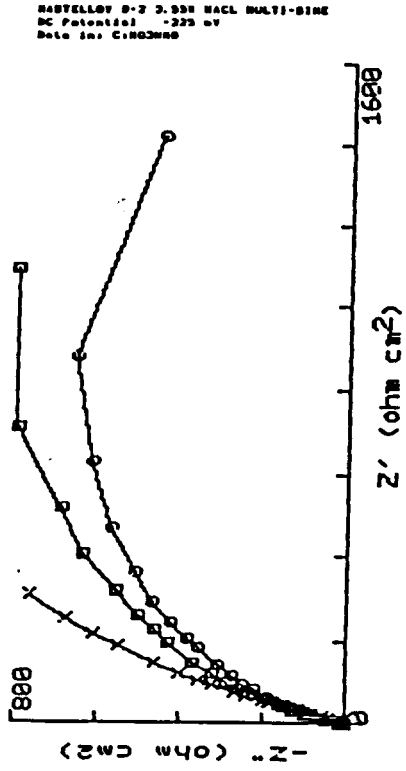
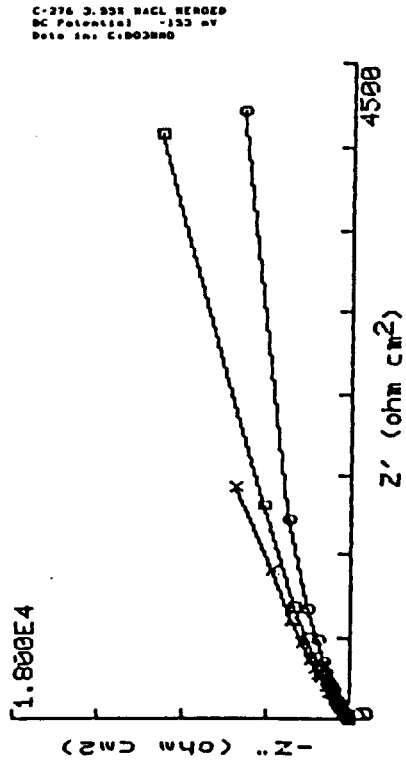
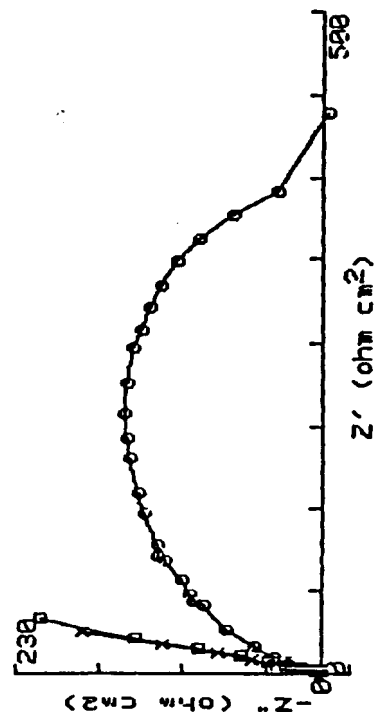
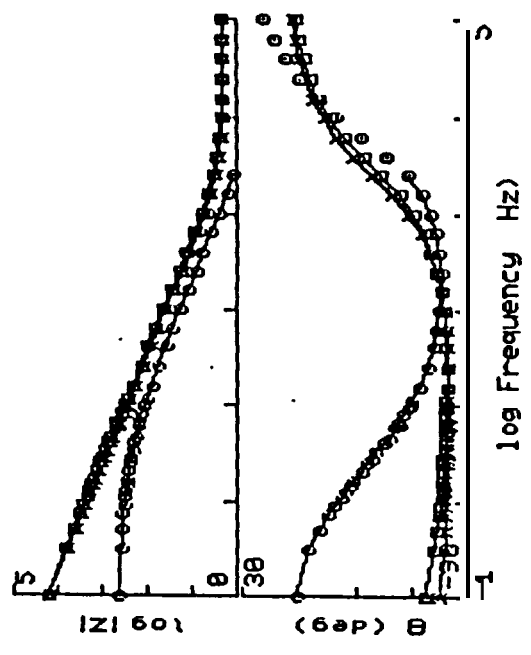


Figure A-4 Nyquist and Bode Plots for Hastelloy C-276 (a,c) and Hastelloy B-2 (b,a)

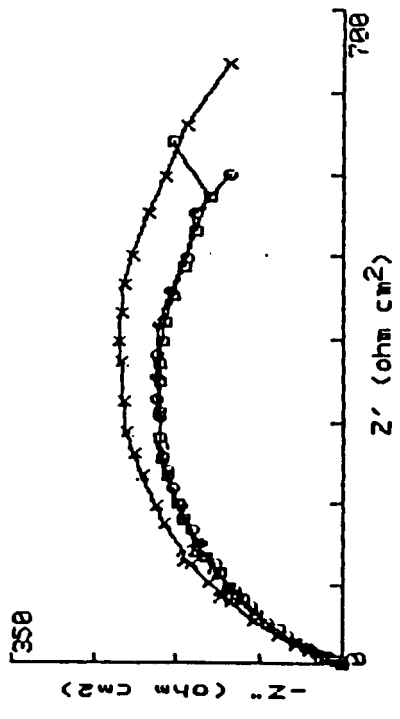
20Cb-3 3.55% NaCl BEADED
 DC Potential: -96 mV
 Date In: C:102686



20Cb-3 3.55% NaCl -1.0M NaCl BEADED
 DC Potential: -272 mV
 Date In: C:102686



MONEL-400 3.55% NaCl -1.0M NaCl BEADED
 DC Potential: -127 mV
 Date In: C:102686



MONEL-400 3.55% NaCl BEADED
 DC Potential: -126 mV
 Date In: C:102686

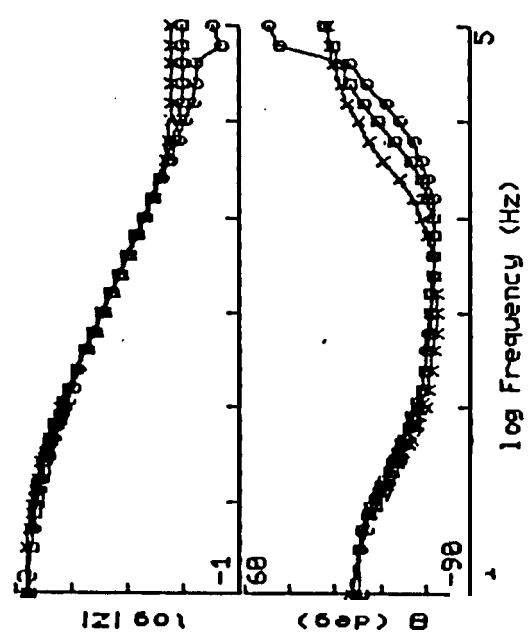


Figure A-5 Nyquist and Bode Plots for Monel ∞ (a,c) a ∞ 20Cb-3 b, ∞

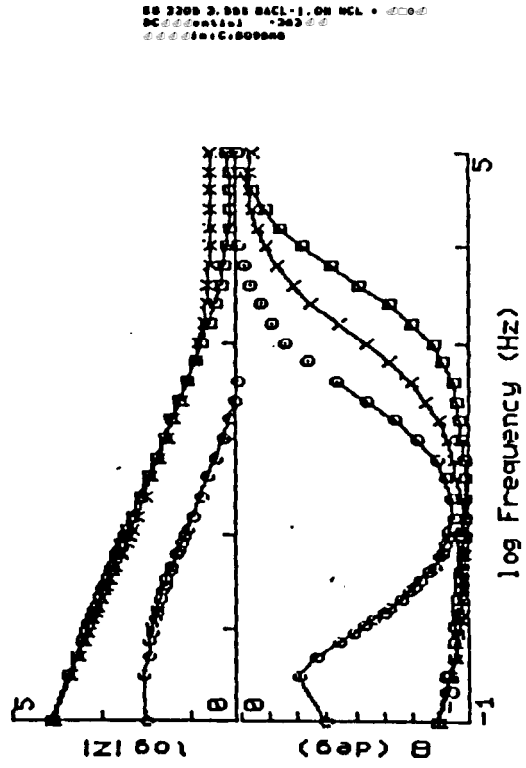
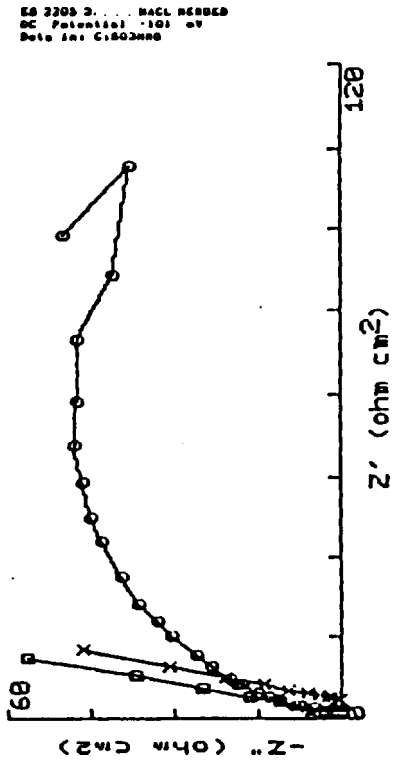
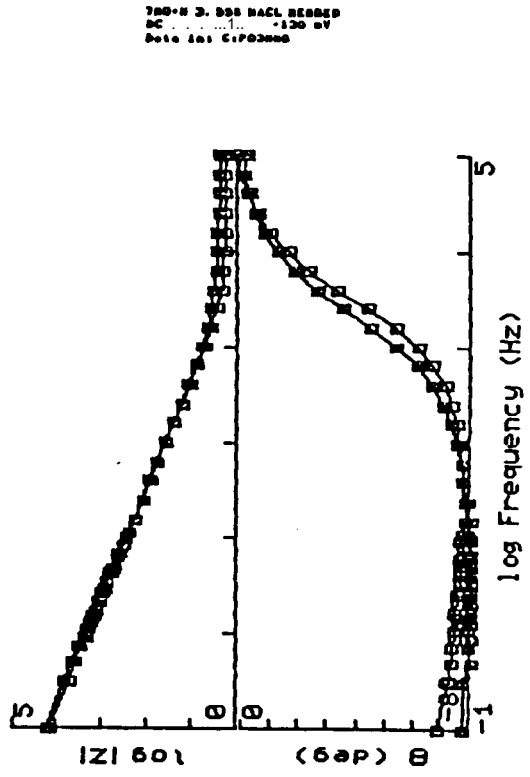
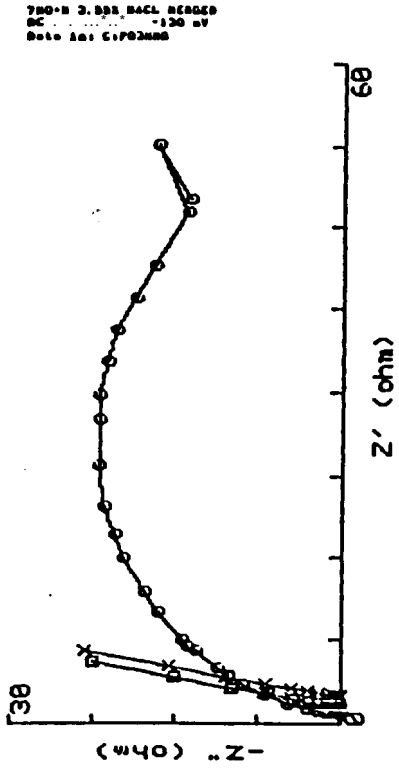


Figure A-6 Nyquist and Bode Plots for ES 2205 (a,c) and 780 + N (b,d)

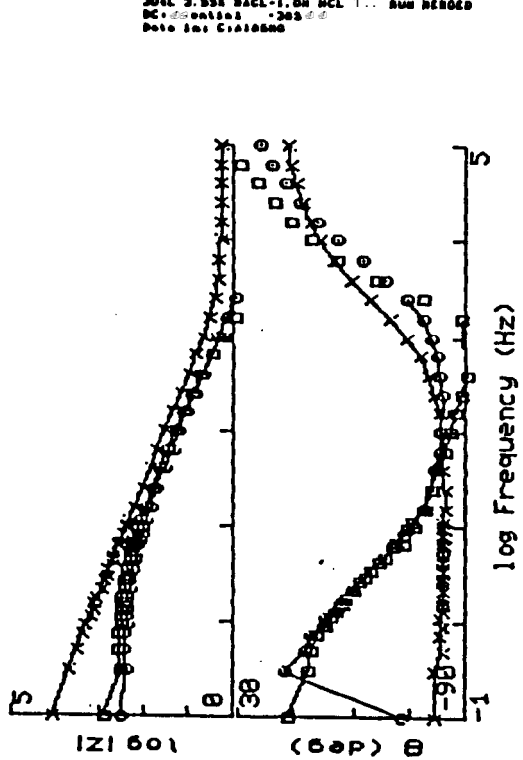
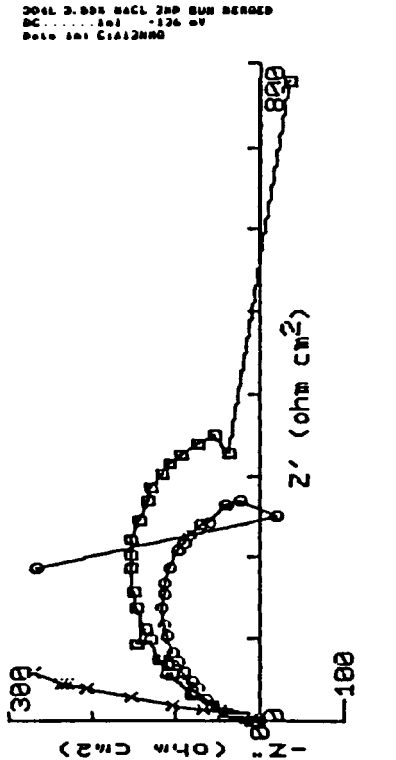
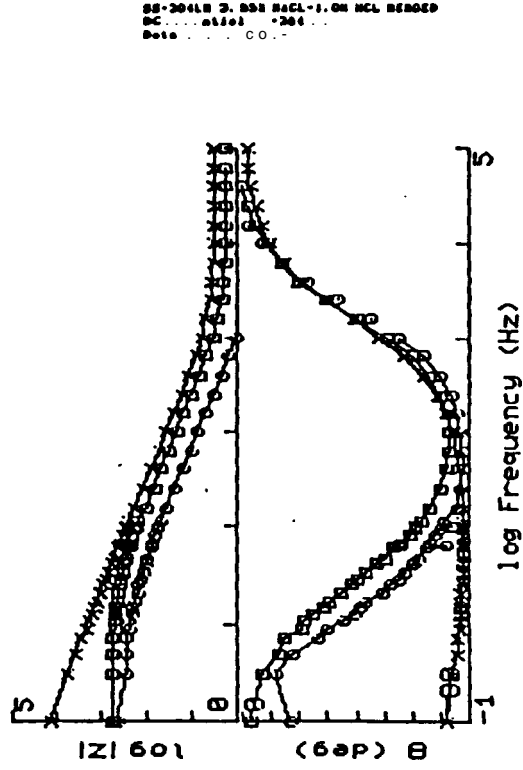
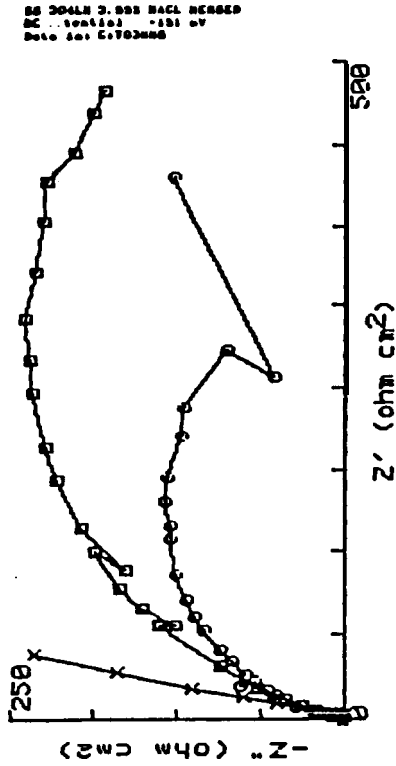
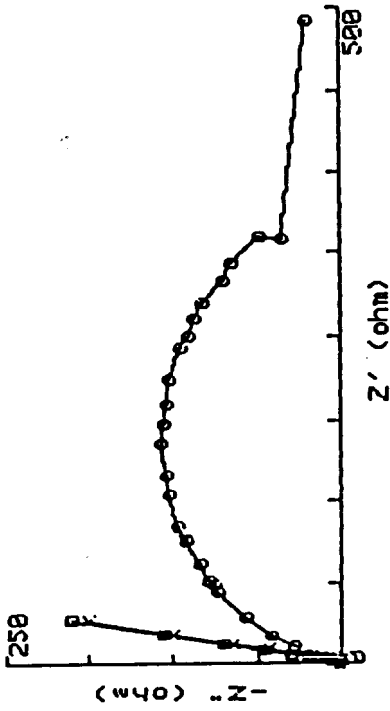
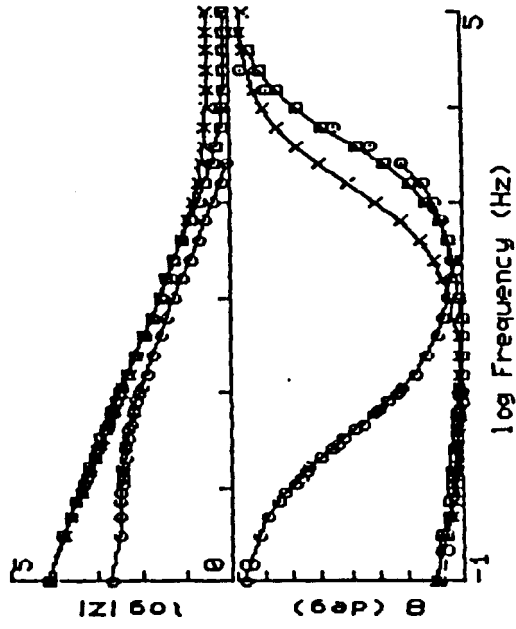


Figure A-7 Nyquist and Bode Plots for SS 304L (a,c) and SS 304LN (b,d)

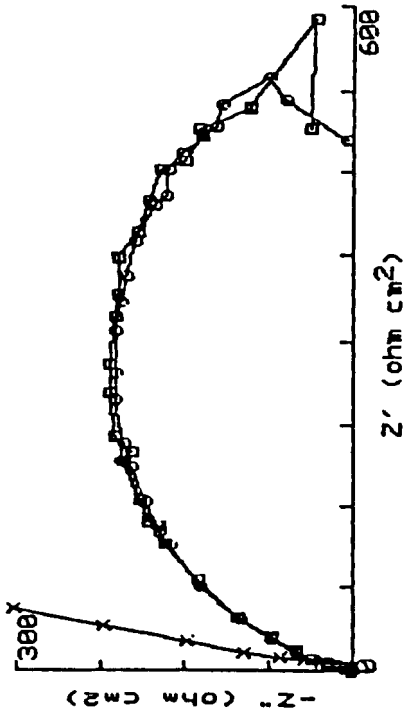
1-625 3.055 NaCl SERVED
 DC Potential -225 mV
 Data for C:002000



1-625 3.055 NaCl-1.0M NaCl SERVED
 DC Potential -225 mV
 Data for C:002000



1-600 3.055 NaCl SERVED
 DC Potential -225 mV
 Data for C:002000



1-600 3.055 NaCl-1.0M NaCl SERVED
 DC Potential -225 mV
 Data for C:002000

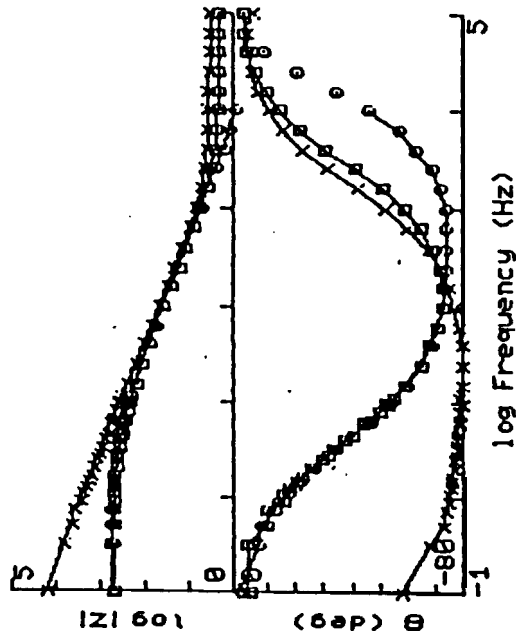


Figure A-8 Nyquist and Bode Plots for Inconel 600 (a,c) and Inconel 825 (b,d)

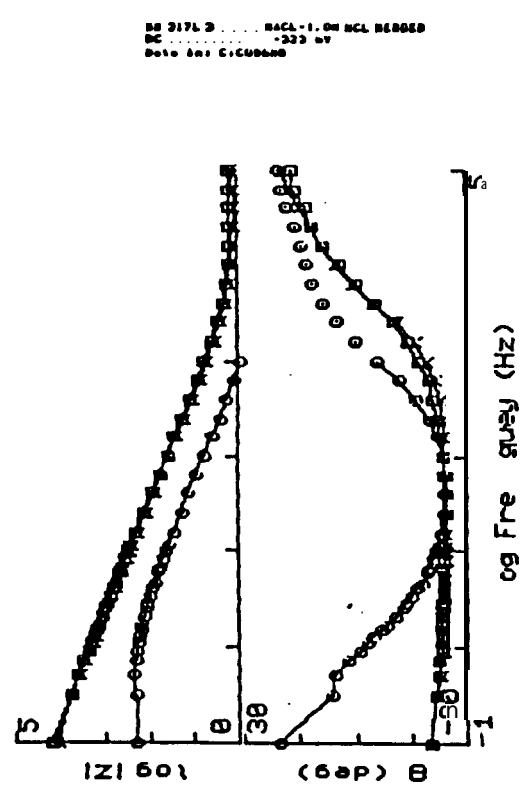
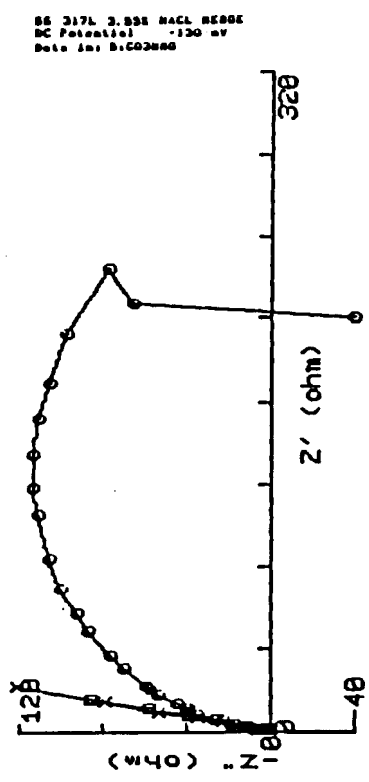
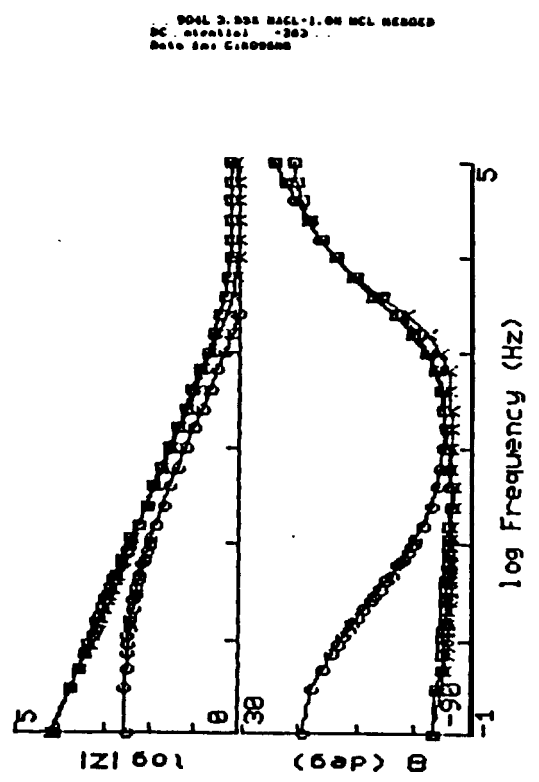
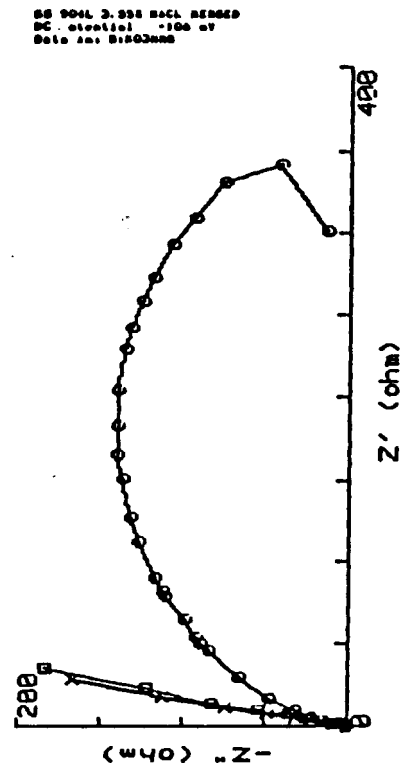
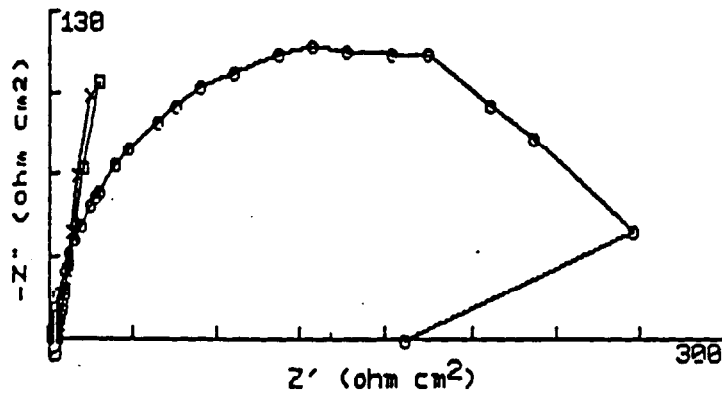
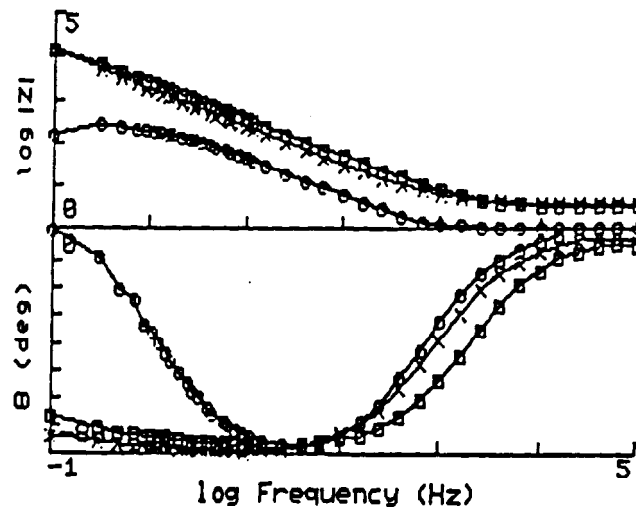


Figure A-9 Nyquist and Bode Plots for SS 317L (a,c) and SS 904L (b,d)



SS 316L 3.000 RCL REFERENCE
R Potential -0.250 V
Rate 100 cm/decade



SS 316L 3.000 RCL REFERENCE
R Potential -0.250 V
Rate 100 cm/decade

Figure A-10 Nyquist and Bode Plots for SS 316L (a,b)

APPENDIX E

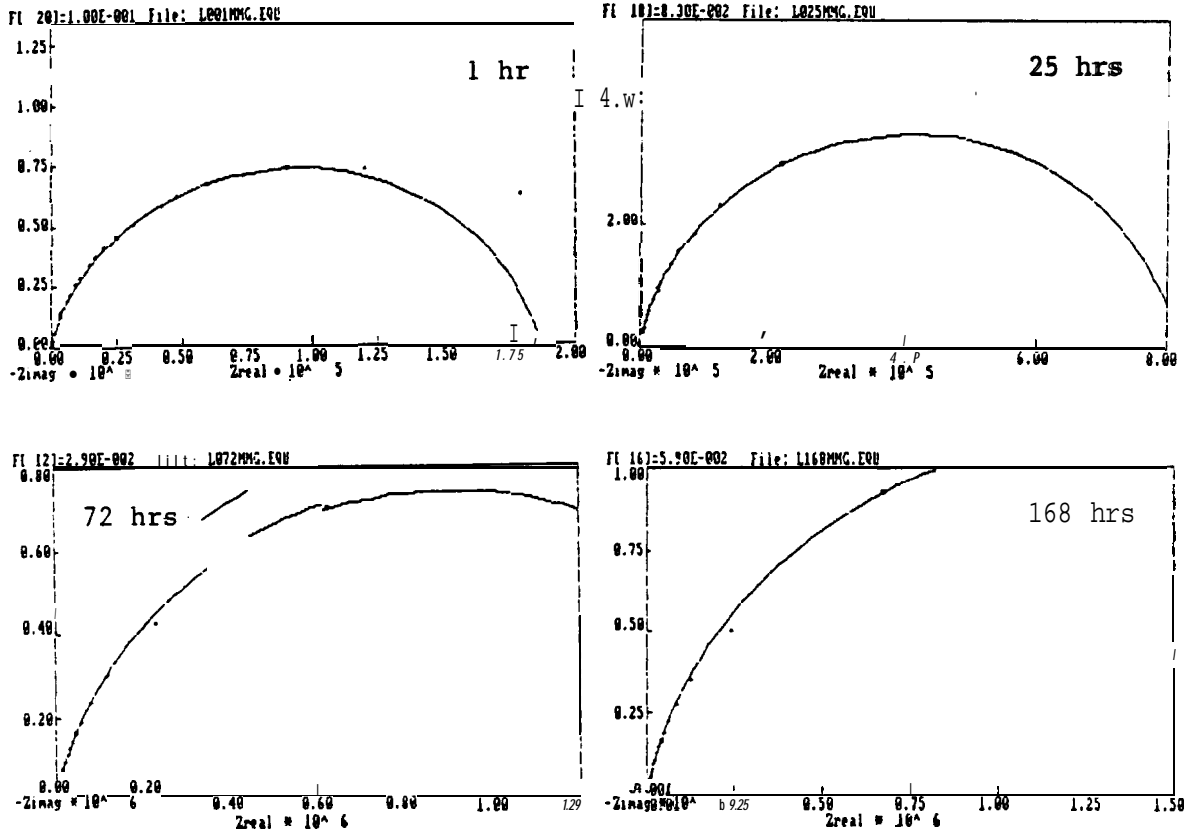


Figure B-1 Nyquist Plots for Hastelloy C-4 in 3.55% NaCl-0.1N HCl at Various Immersion Times

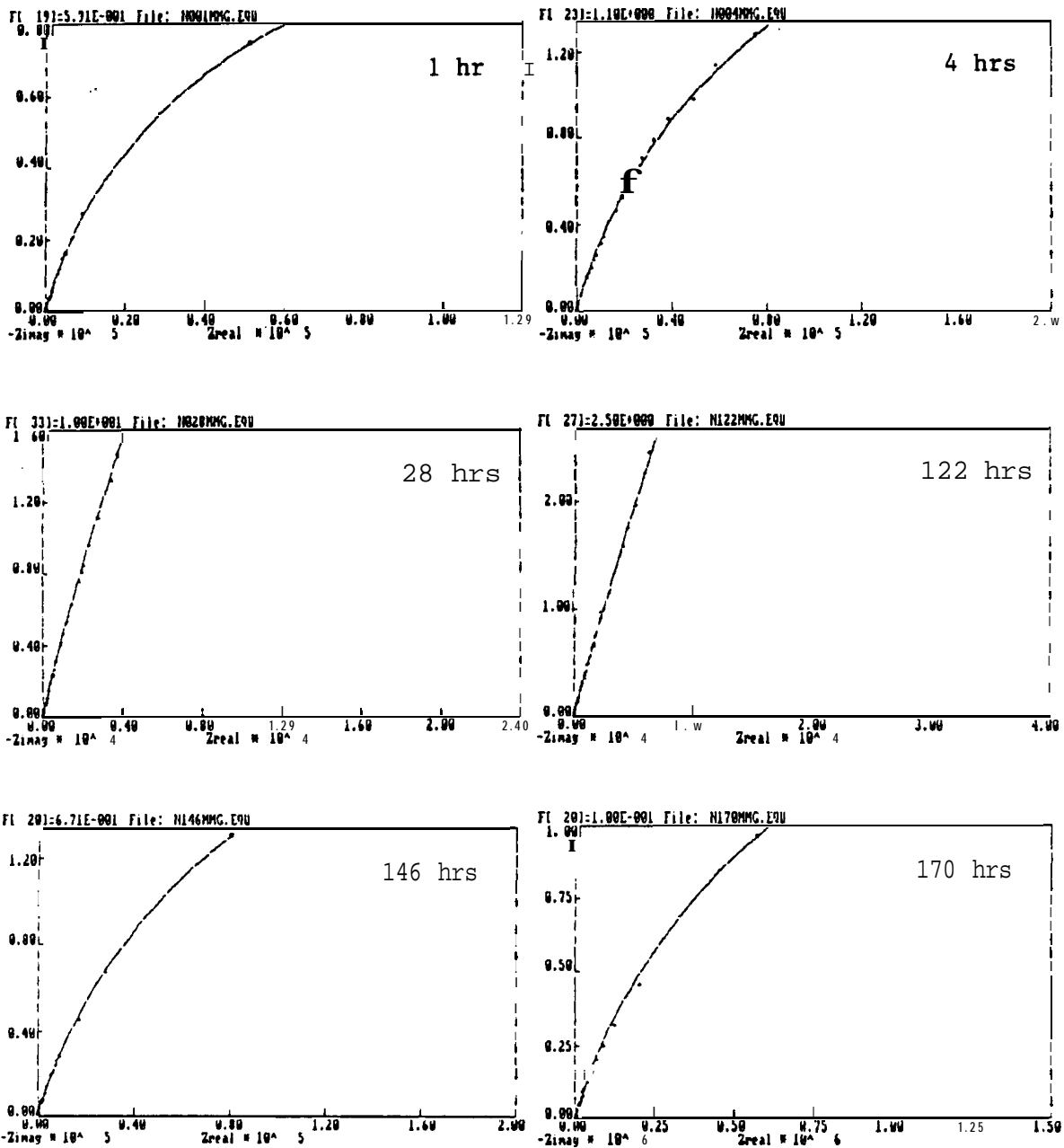


Figure B-2 Nyquist Plots for Hastelloy C-22 in 3.55% NaCl-0.1N HCl at Various Immersion Times

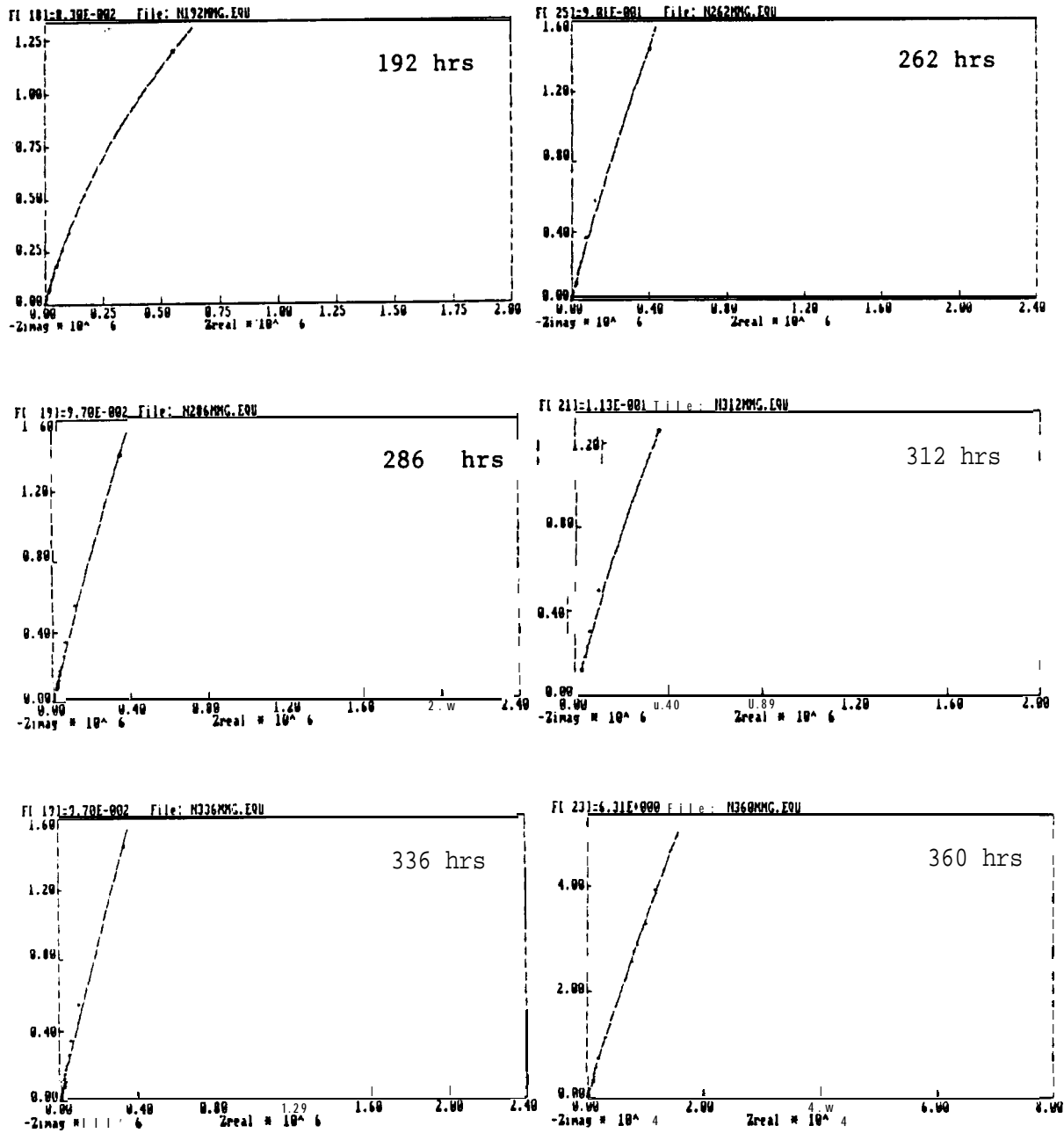


Figure B-2 (Cont)

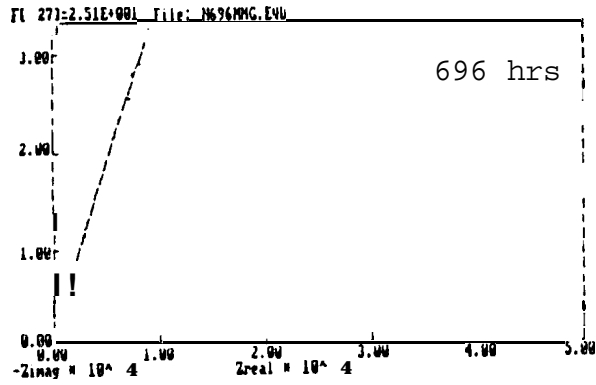
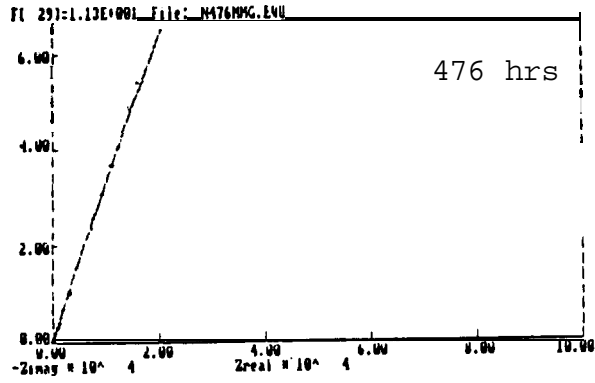


Figure B-2 (Cont)

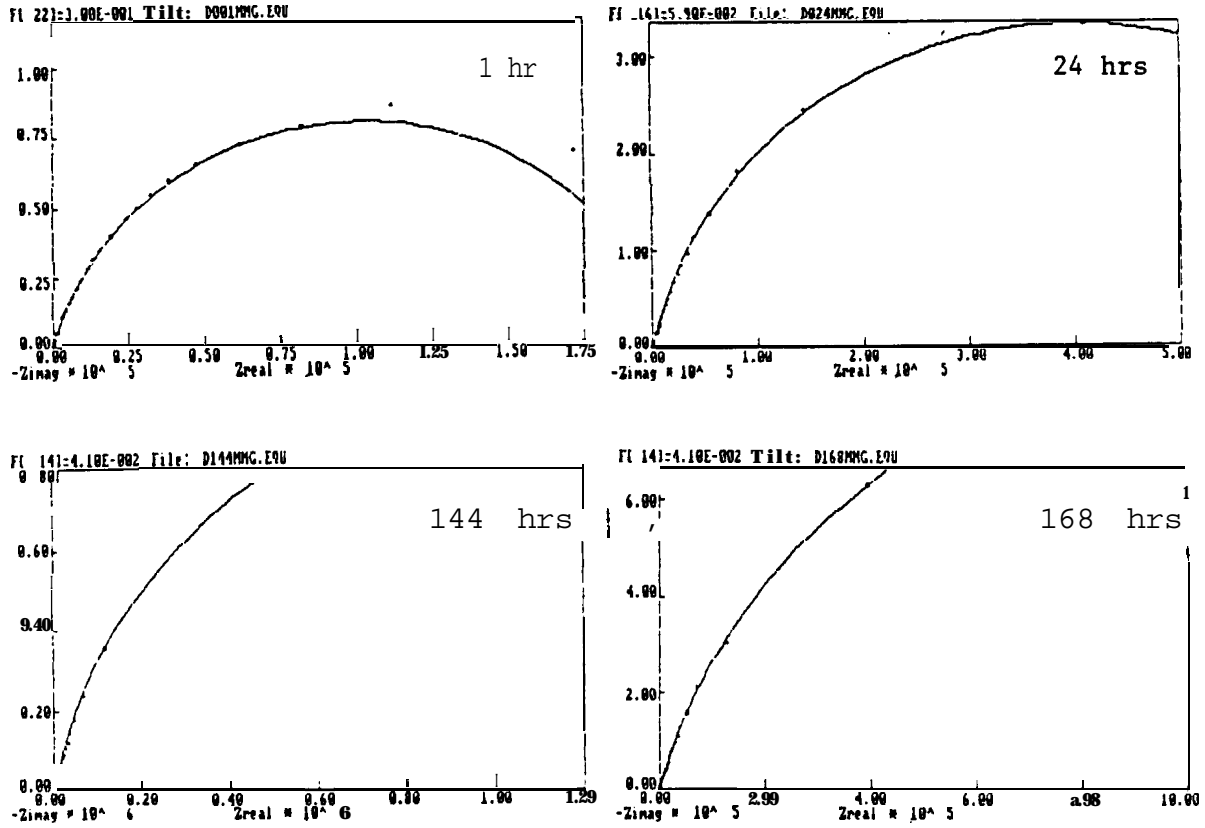


Figure B-3 Nyquist Plots for Hastelloy C-276 in 3.55% NaCl-0.1N HCl at Various Immersion Times

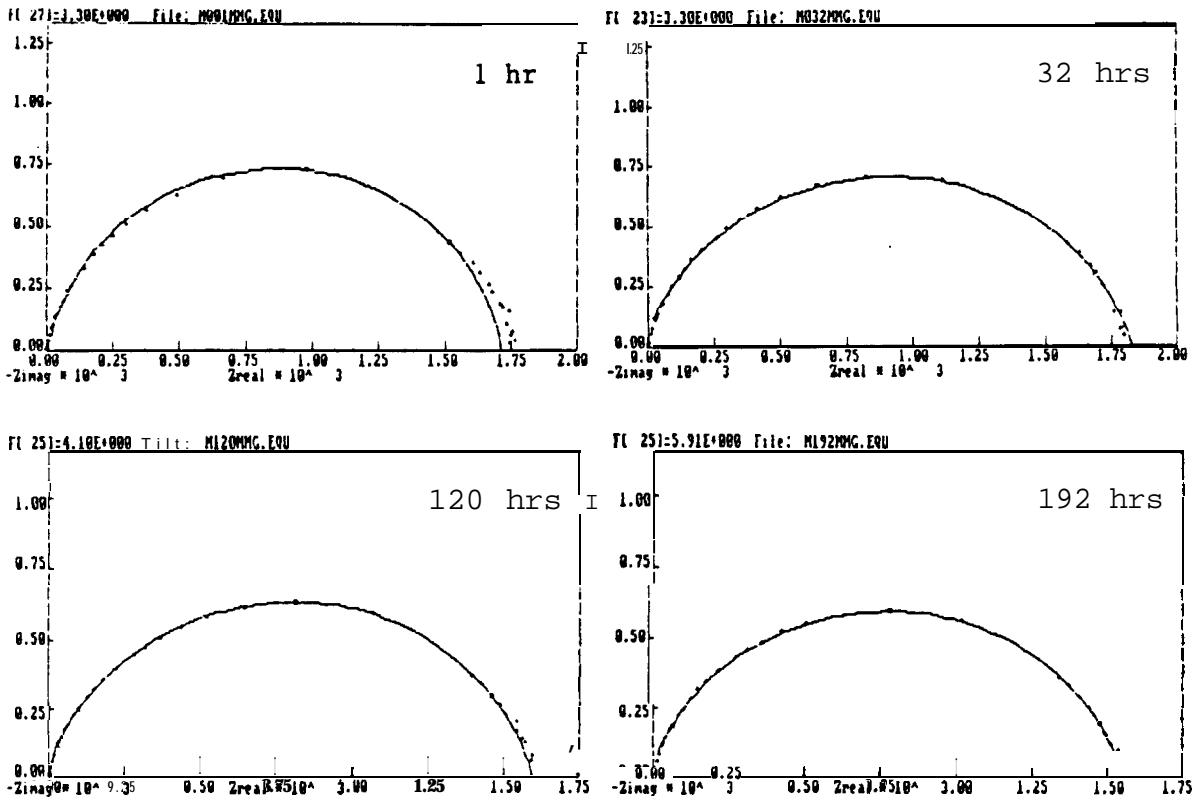


Figure B-4 Nyquist Plots for Hastelloy B-2 in 3.55% NaCl-0.1N HCl at Various Immersion Times

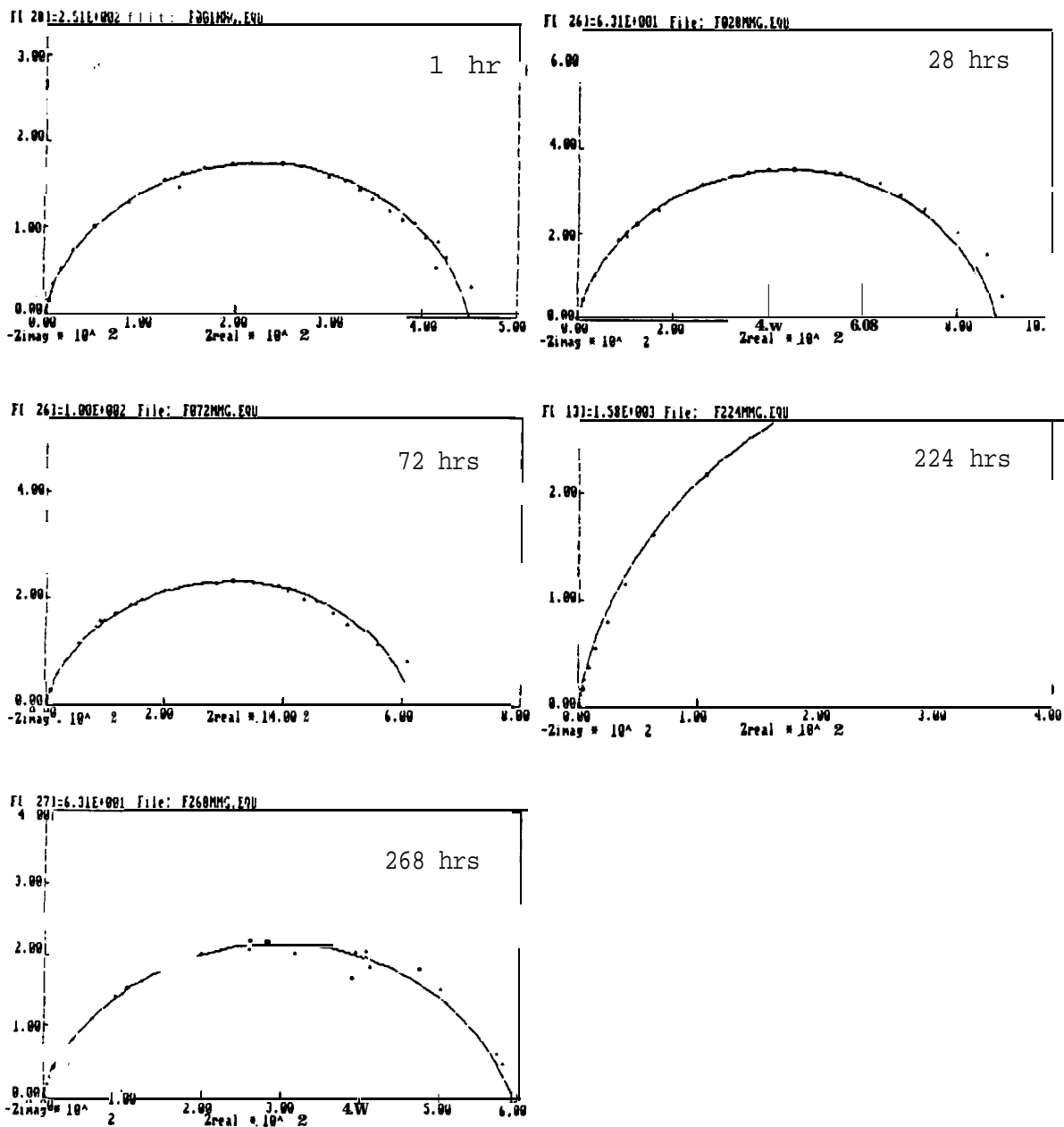


Figure B-5 Nyquist Plots for Inconel 600 in 3.55% NaCl-0.1N HCl at Various Immersion Times

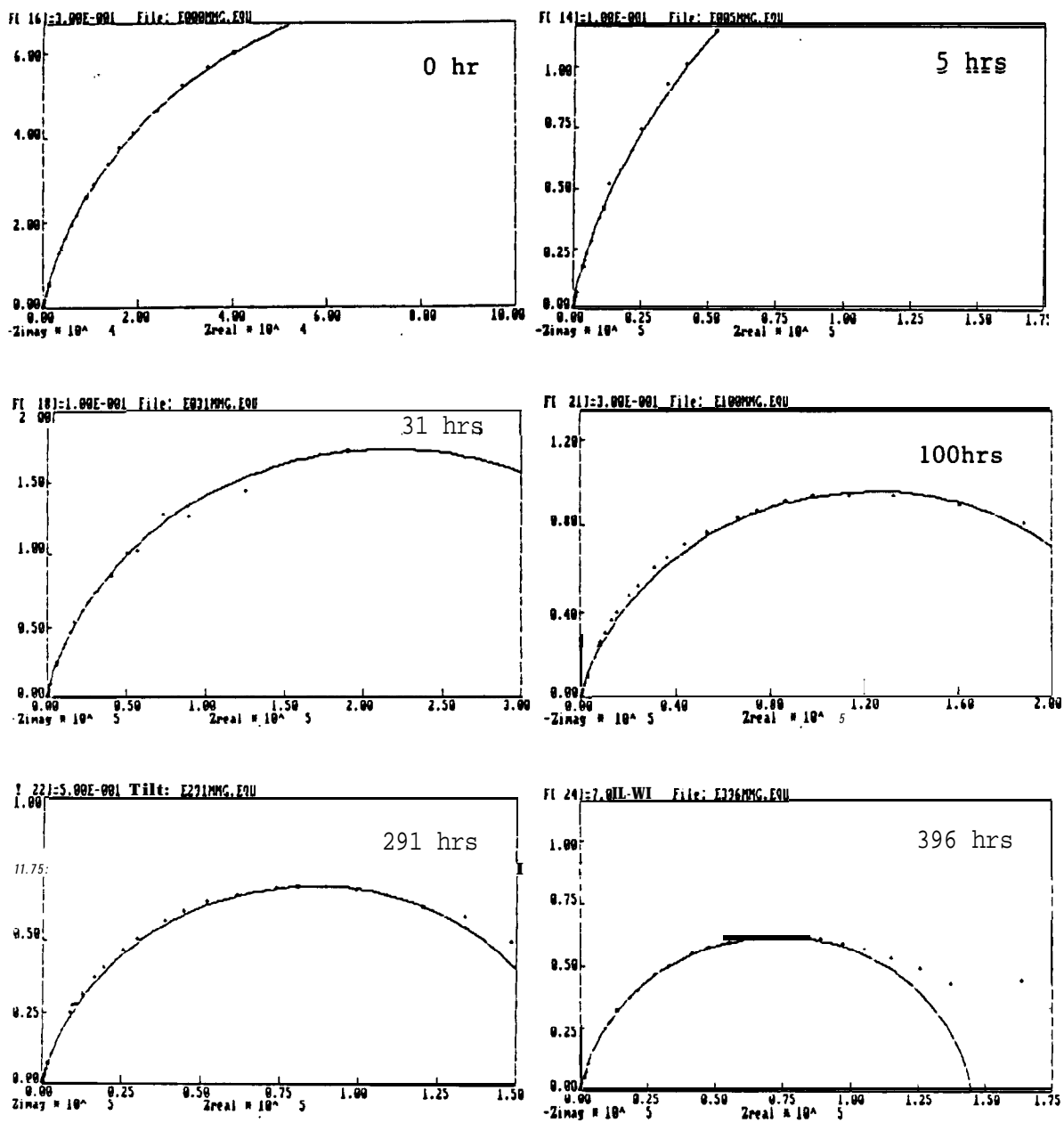


Figure B-6 Nyquist Plots for Inconel 625 in 3.55% NaCl-0.1N HCl at Various Immersion Times

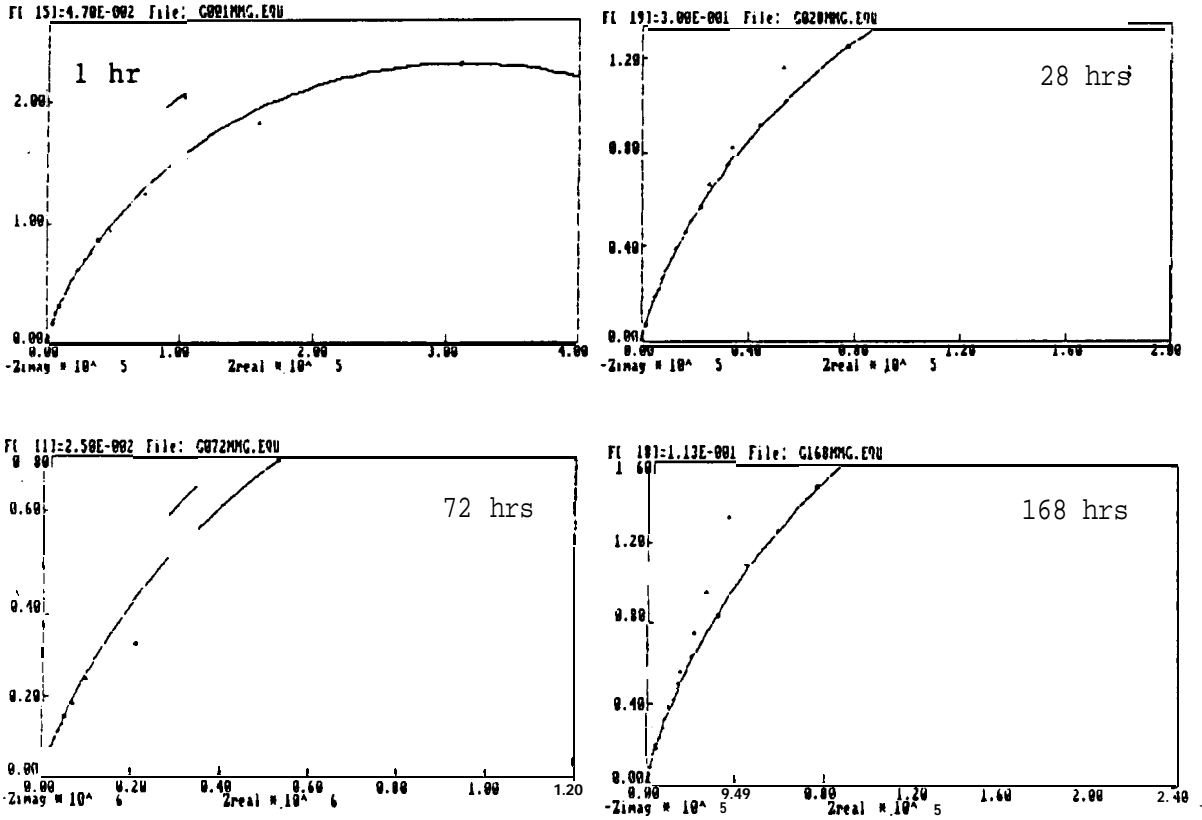


Figure B-7 Nyquist Plots for Inconel 825 in 3.55% NaCl-0.1N HCl at Various Immersion Times

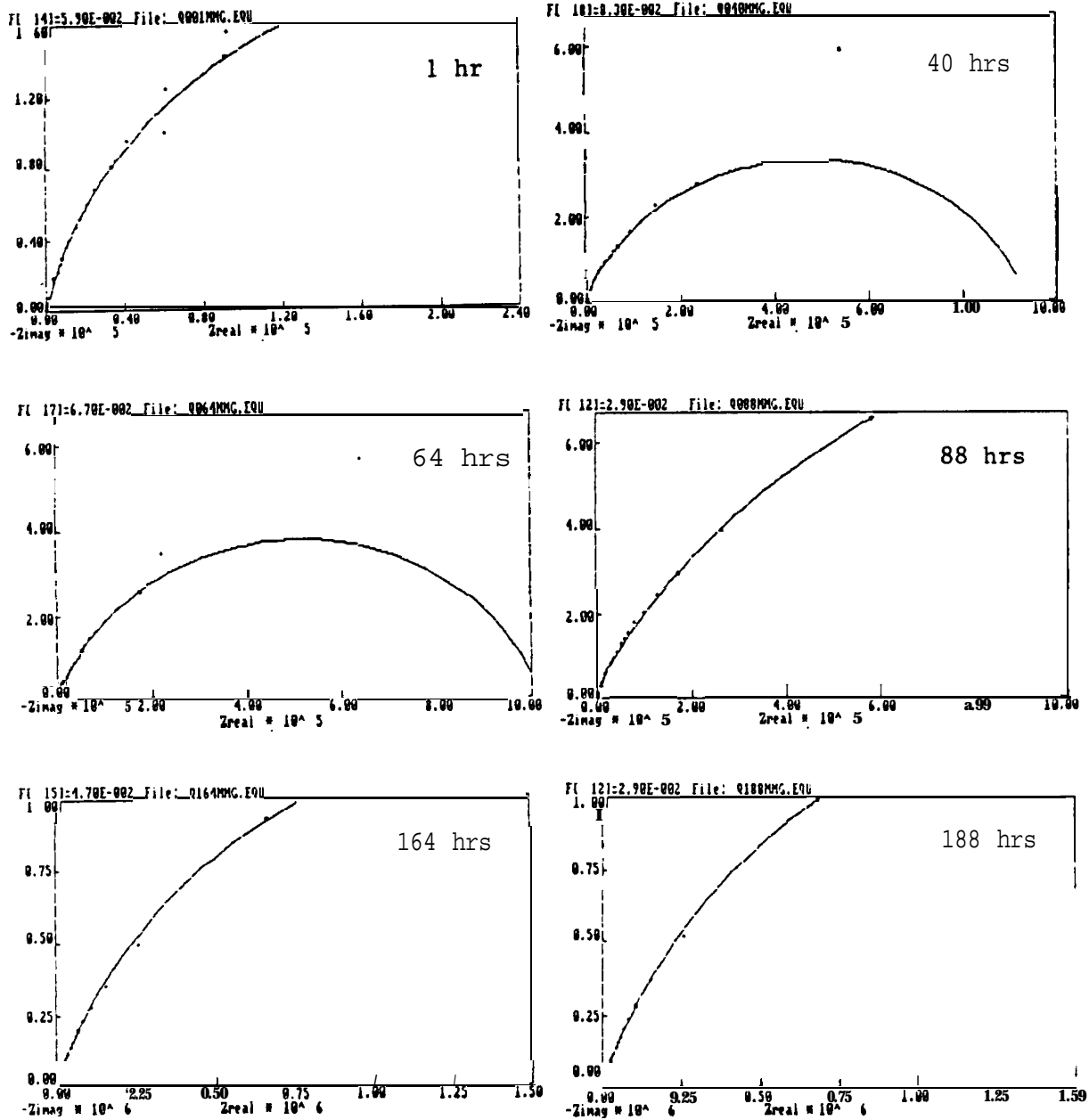


Figure B-8 Nyquist Plots for Inco G-3 in 3.55% NaCl-0.1N HCl at Various Immersion Times

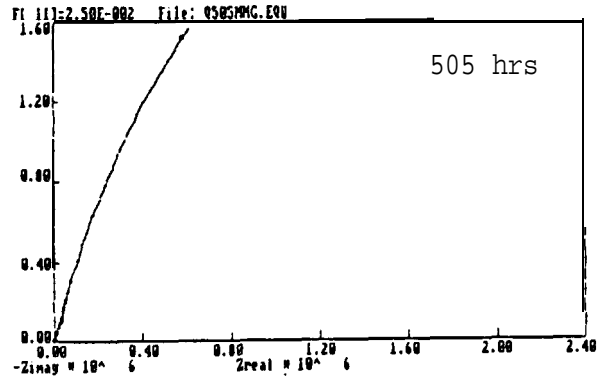
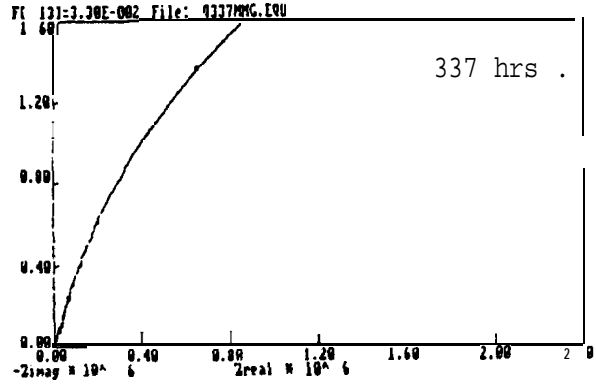


Figure B-8 (Cont)

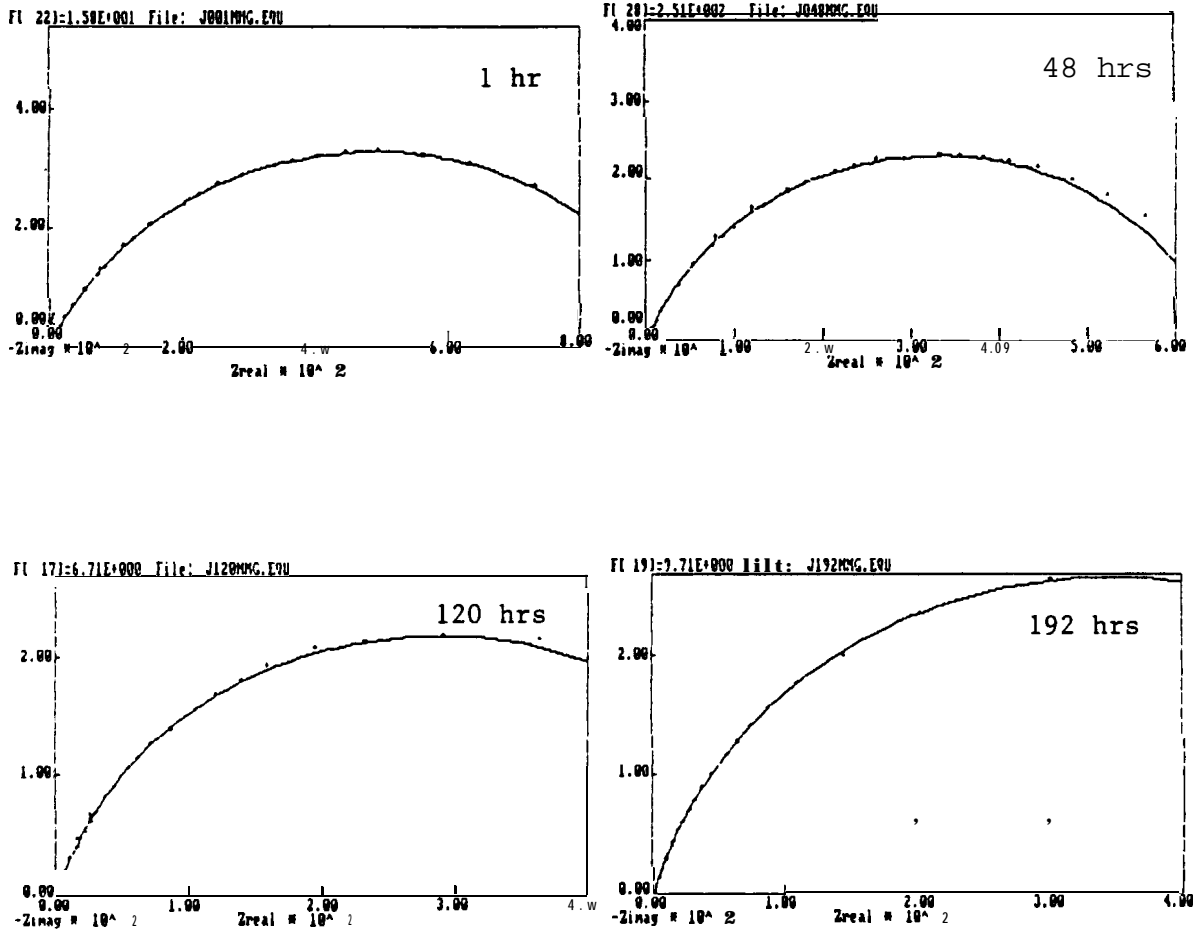


Figure B-9 Nyquist Plots for Monel 400 in 3.55% NaCl-0.1N HCl at Various Immersion Times

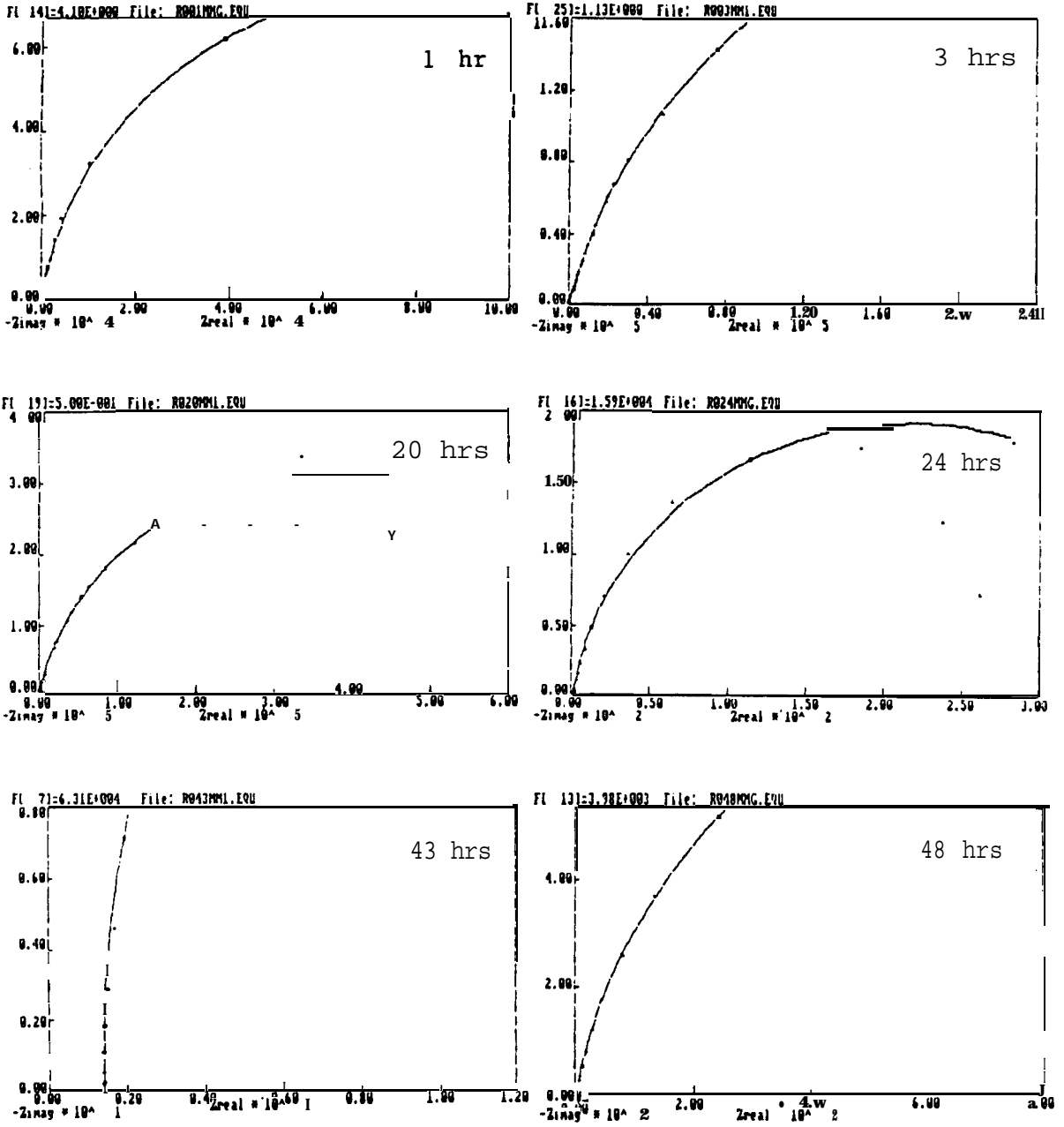


Figure B-10 Nyquist Plots for Zirconium 702 in 3.55% NaCl-0.1N HCl in Various Immersion Times

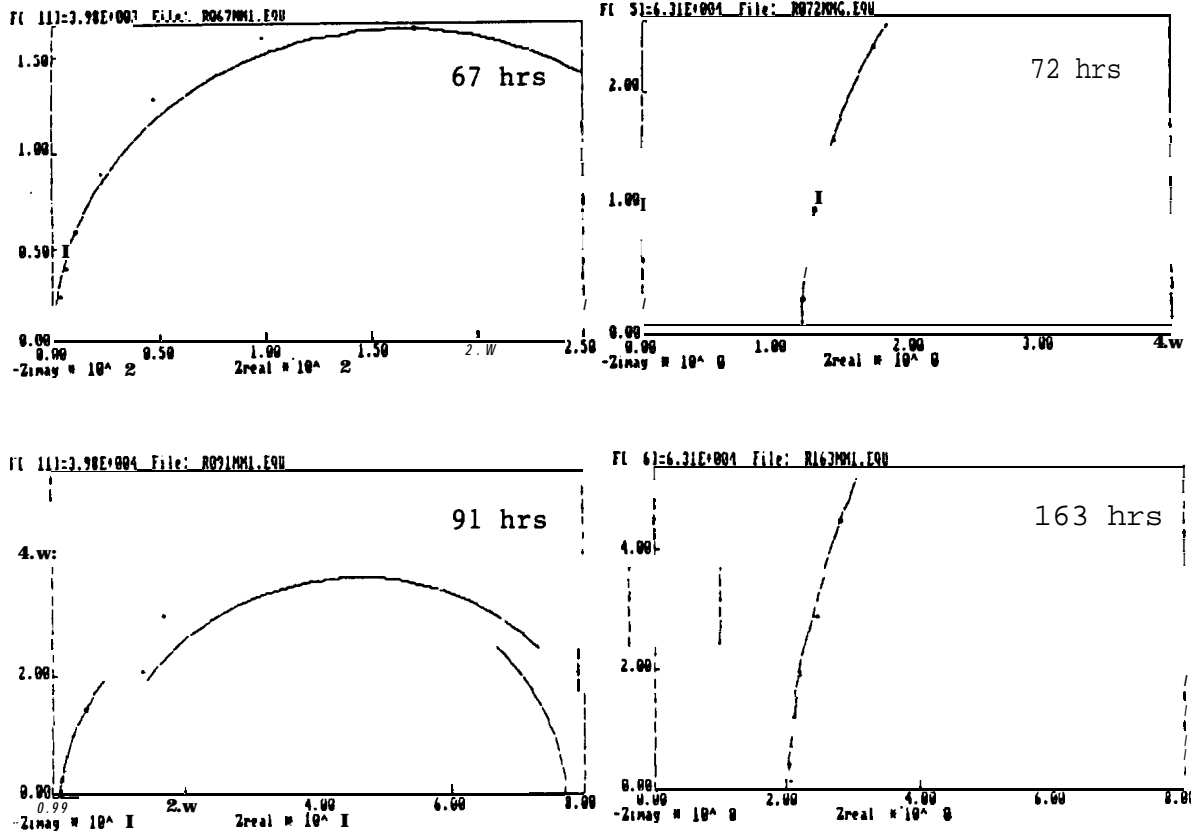


Figure B-10 (Cont)

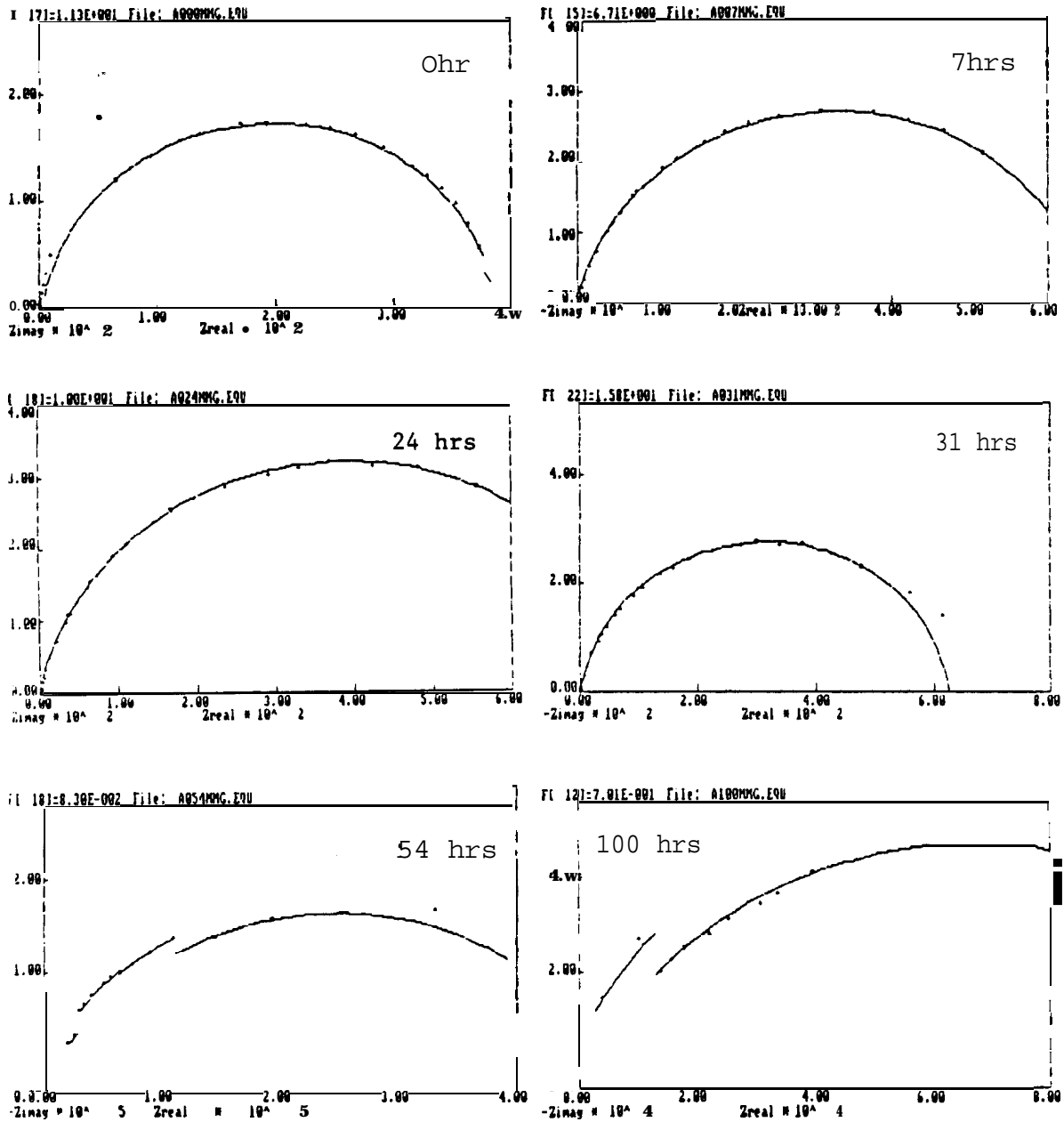


Figure B-11 Nyquist Plots for SS 304L in 3.55% NaCl-0.1N HCl at Various Immersion Times

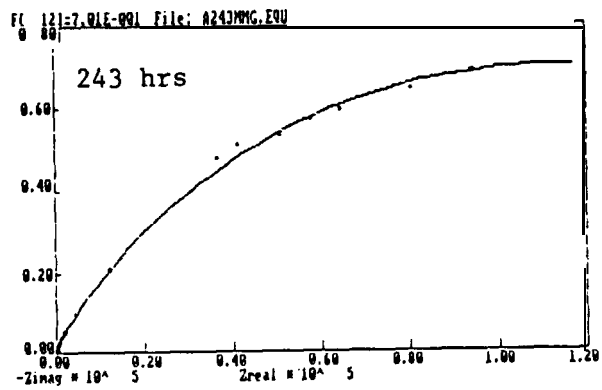
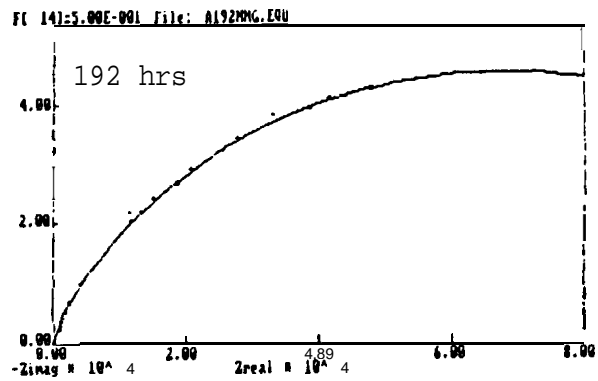
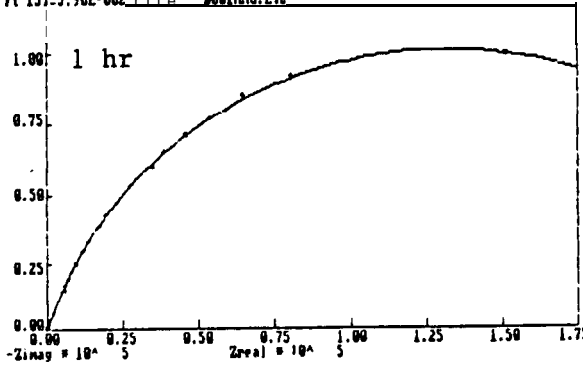
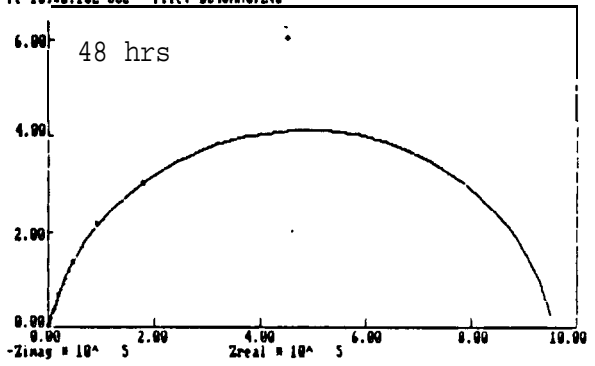


Figure B-11 (Cont)

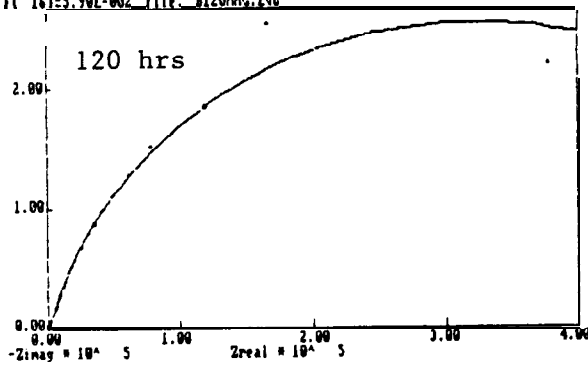
Fl 151:5.90E-002 File: D001MMG.EQU



Fl 101:2.10E-002 File: D040MMG.EQU



Fl 161:5.90E-002 File: D120MMG.EQU



Fl 141:4.10E-002 File: D192MMG.EQU

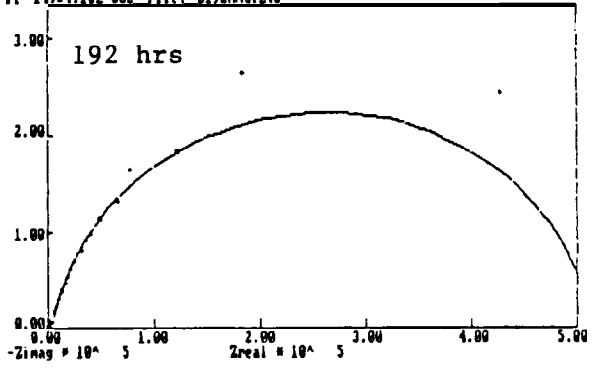


Figure B-12 Nyquist Plots for SS 316L in 3.55% NaCl-0.1N HCl at Various Immersion Times

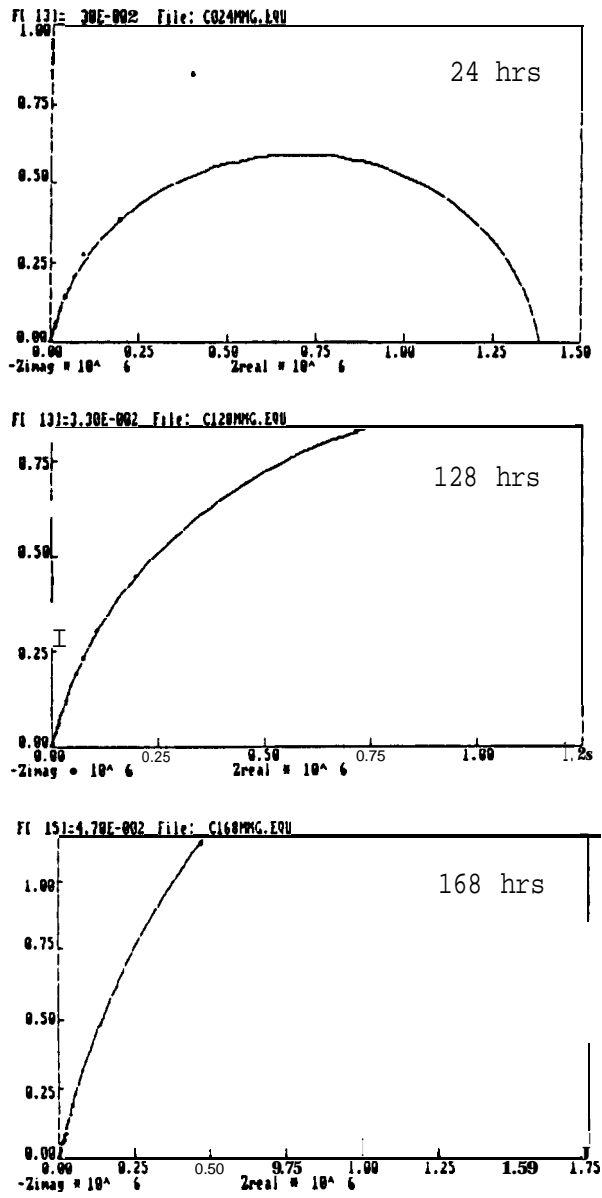


Figure B-13 Nyquist Plots for SS 317L in 3.55% NaCl-0.1N HCl at Various Immersion Times

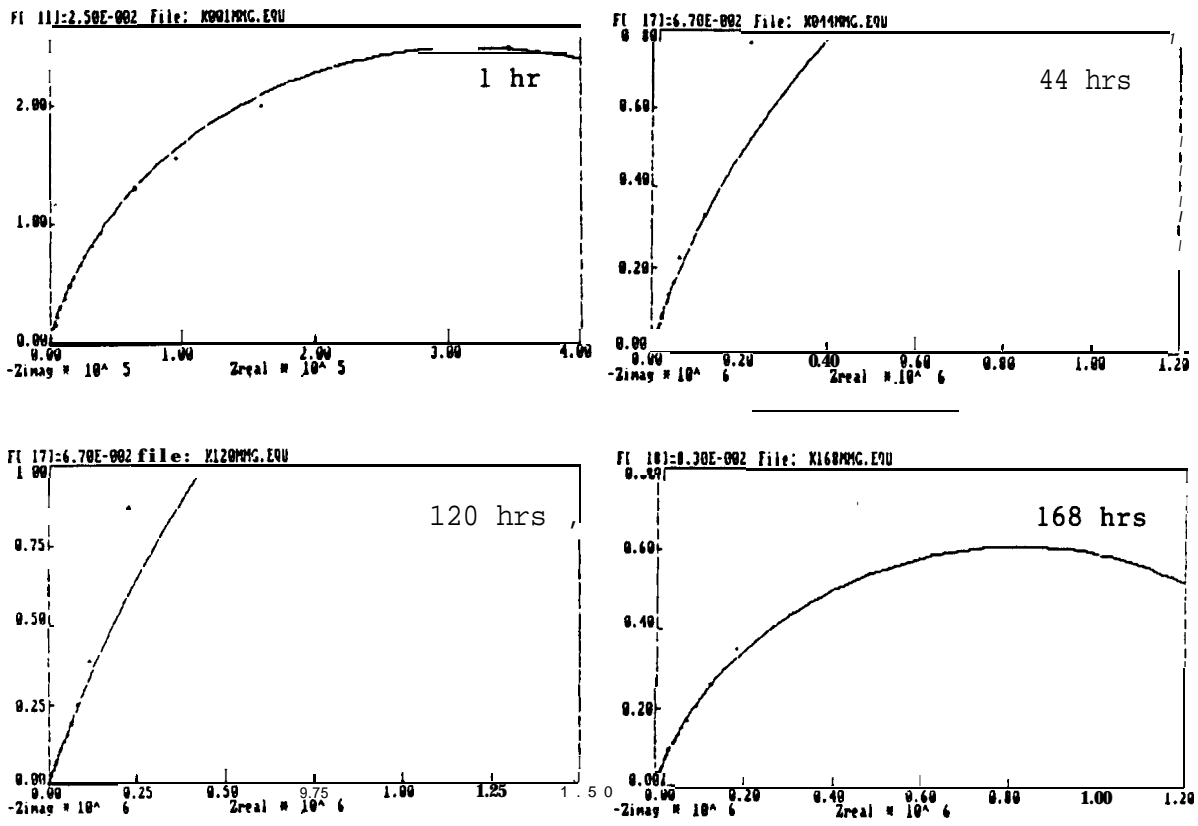


Figure B-14 Nyquist Plots for SS 904L in 3.55% NaCl-0.1N HCl at Various Immersion Times

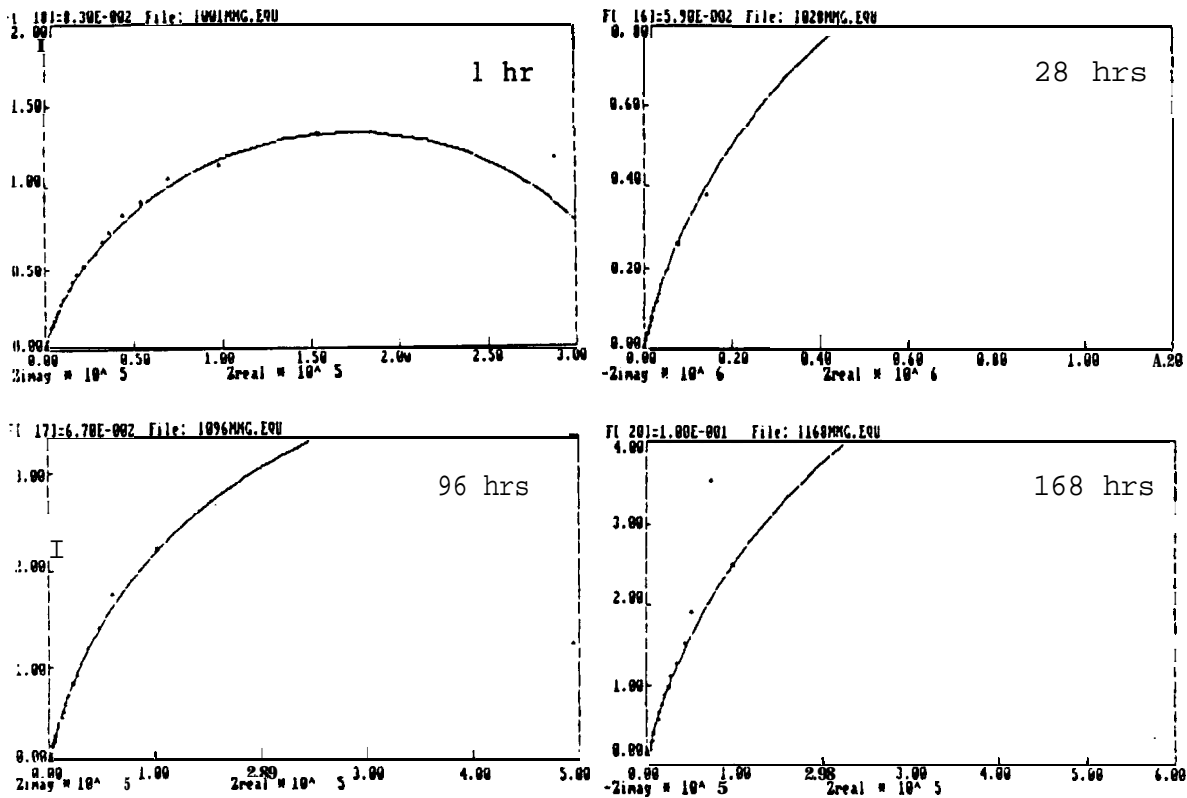


Figure B-15 Nyquist Plots for 20 Cb-3 in 3.55% NaCl-0.1N HCl in Various Immersion Times

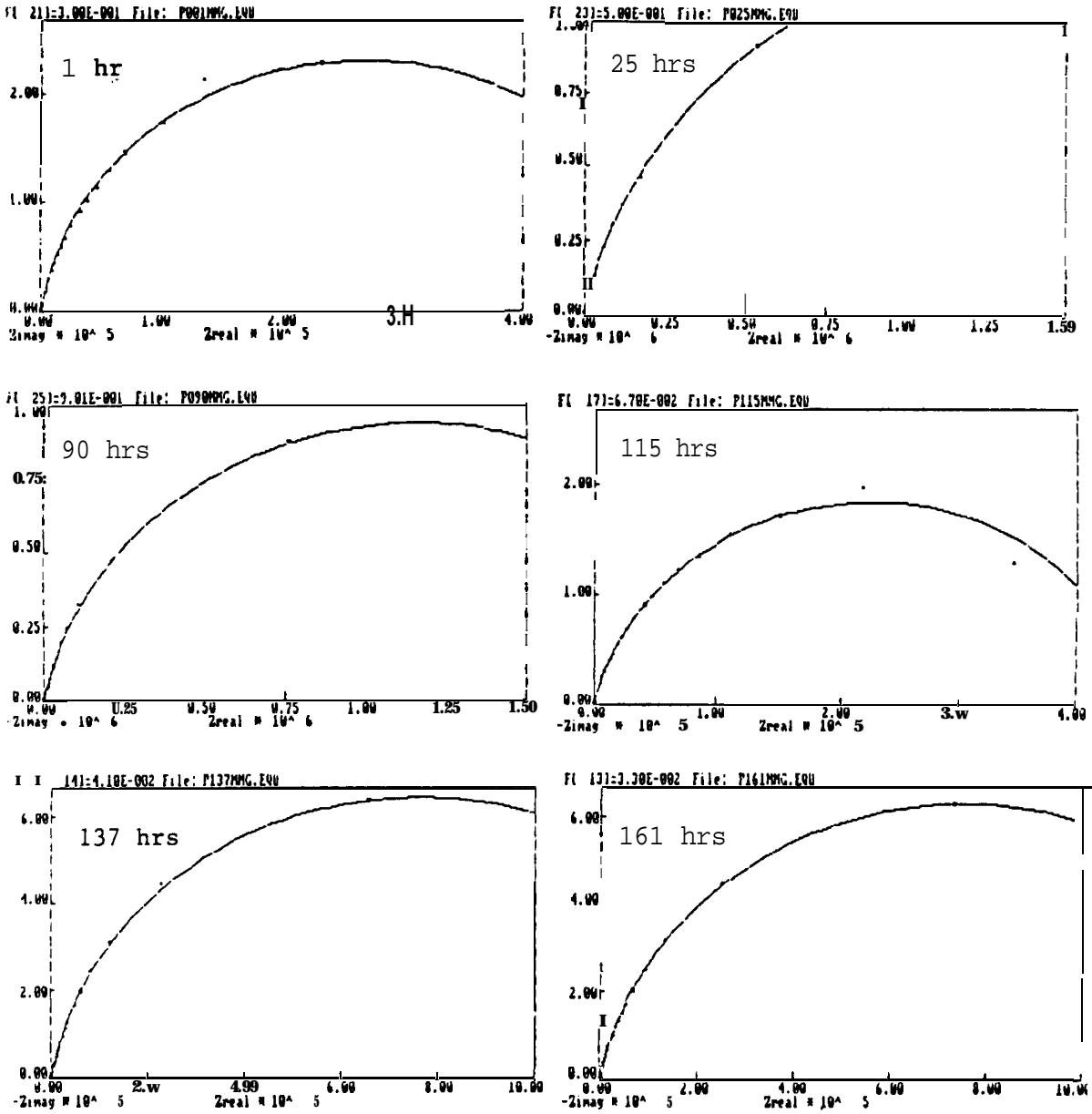


Figure B-16 Nyquist Plots for 7 Mo + N in 3.55% NaCl-0.1N HCl at Various Immersion Times

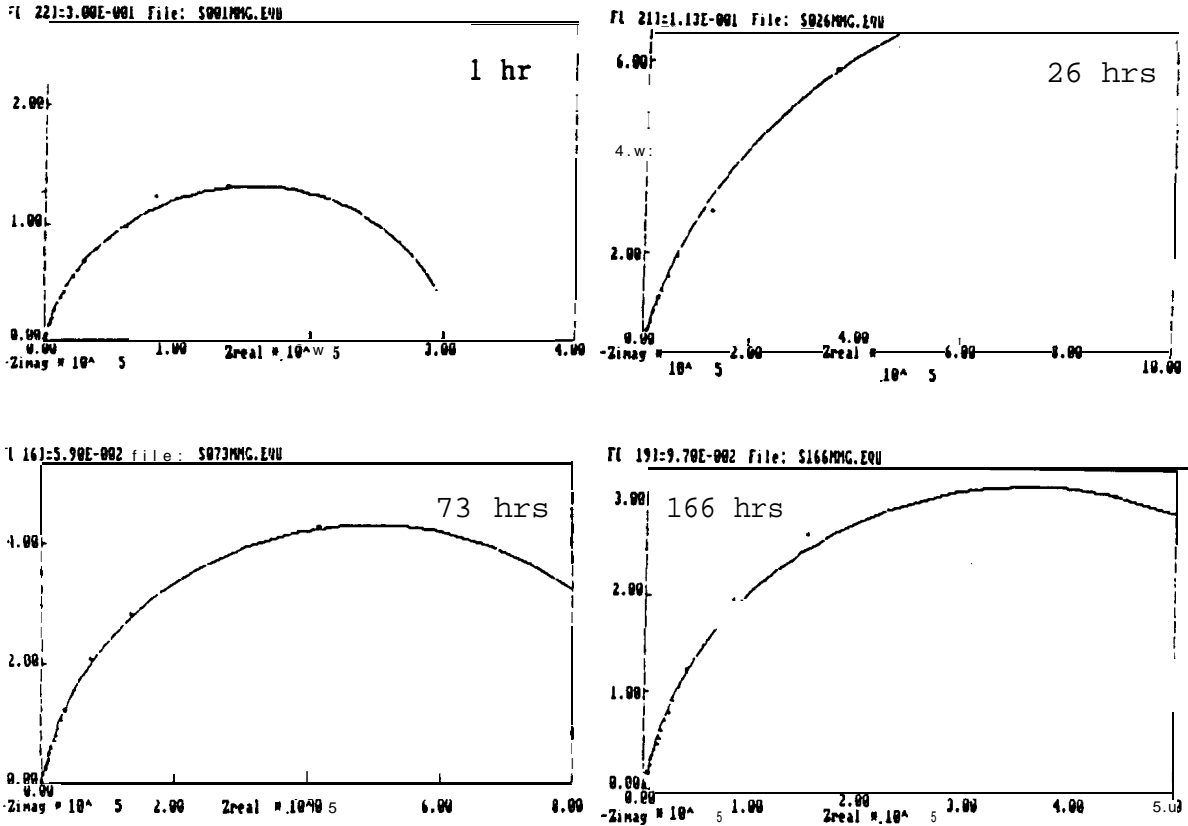


Figure B-17 Nyquist Plots for ES-2205 in 3.55% NaCl-0.1N HCl at Various Immersion Times

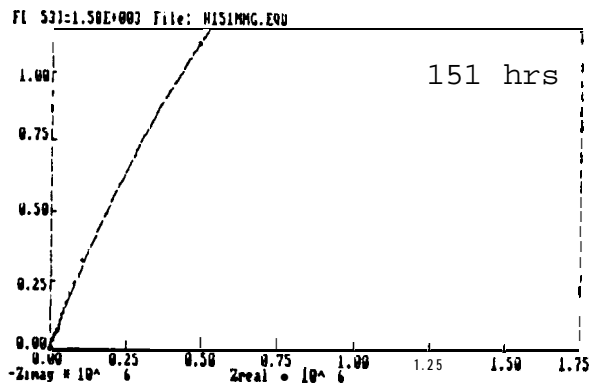
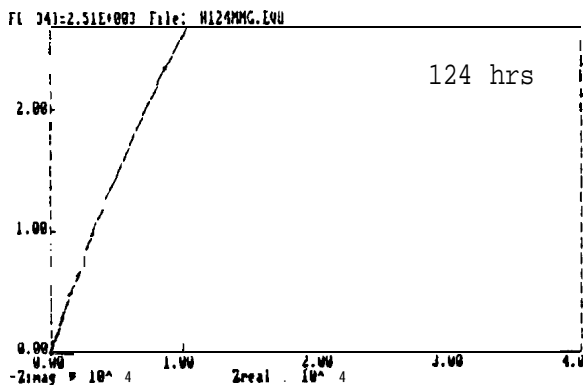
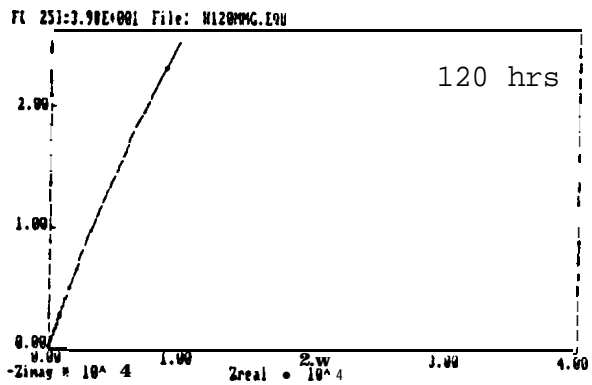
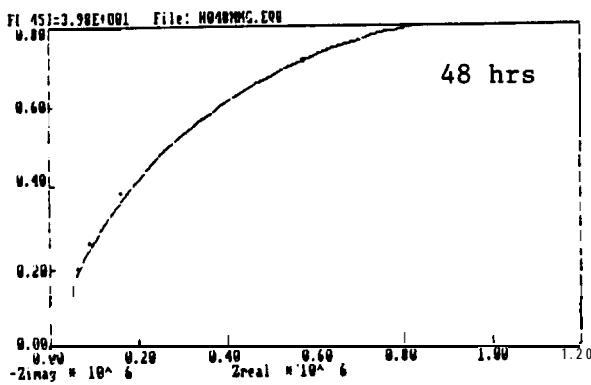
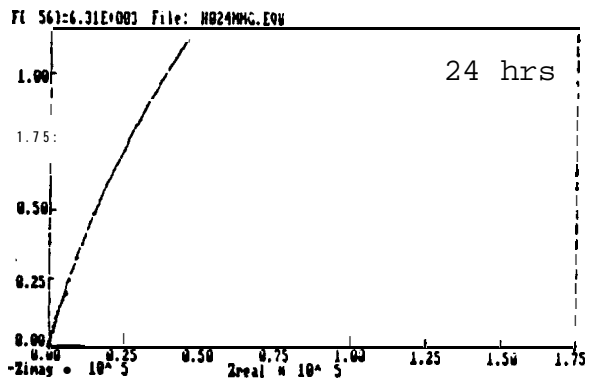
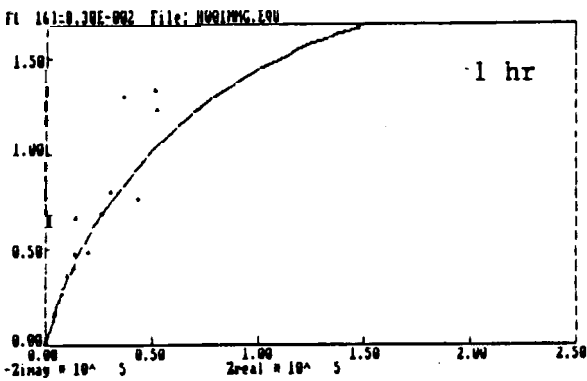


Figure B-18 Nyquist Plots for Ferralum 255 in 3.55% NaCl-0.1N HCl in Various Immersion Times

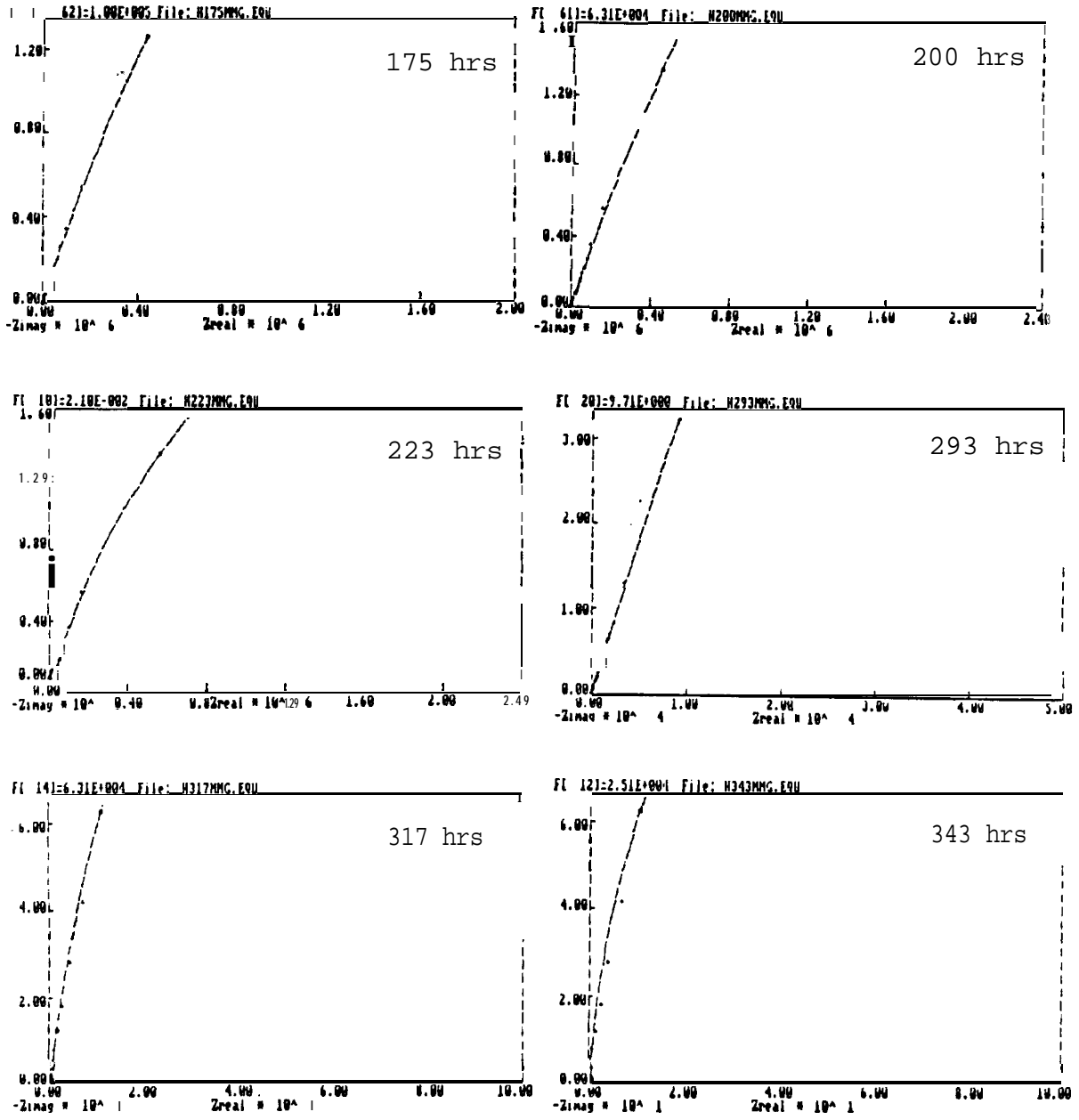


Figure B-18 (Cont)

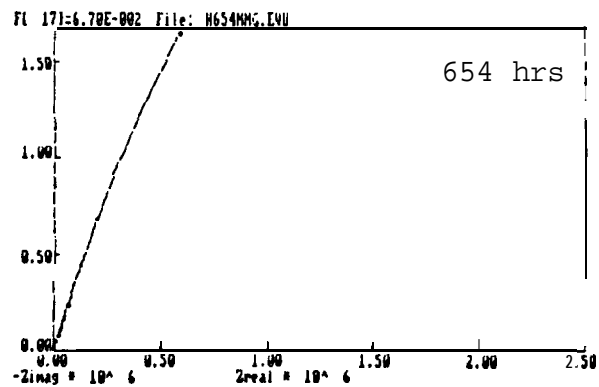
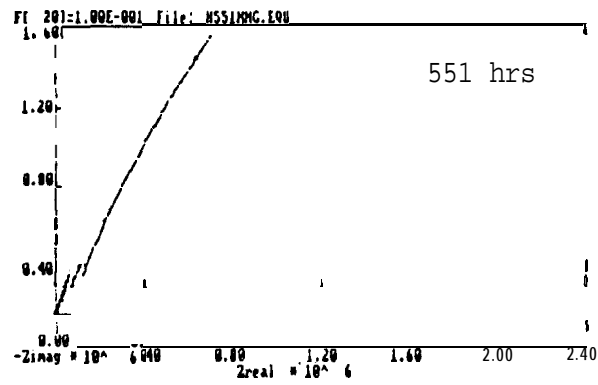
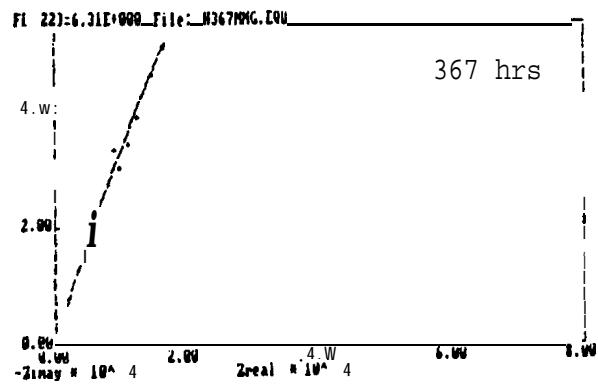


Figure B-18 (Cont)